Sparse Sampling Methods for Large Scale Experimental Data

Rick Archibald
Oak Ridge National Laboratory

IPAM January 2017
Big Data Meets Computation

Outline

- *DOE Facilities*
- *ACUMEN Project*
- Sparse Optimization
  - Tomography
  - Denoising

Motivation – Computation Facilities

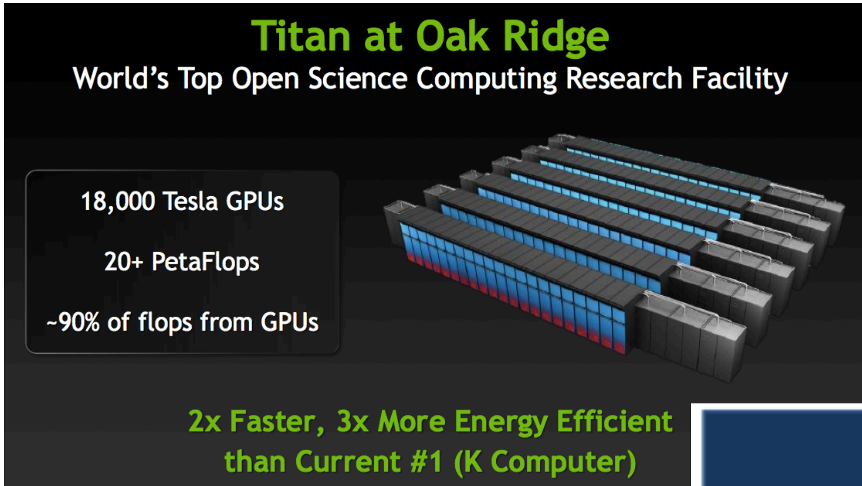

The Free Lunch Is Over: A Fundamental Turn Toward Concurrency in Software

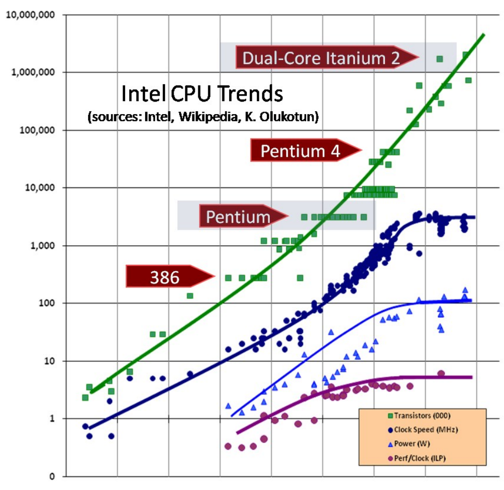

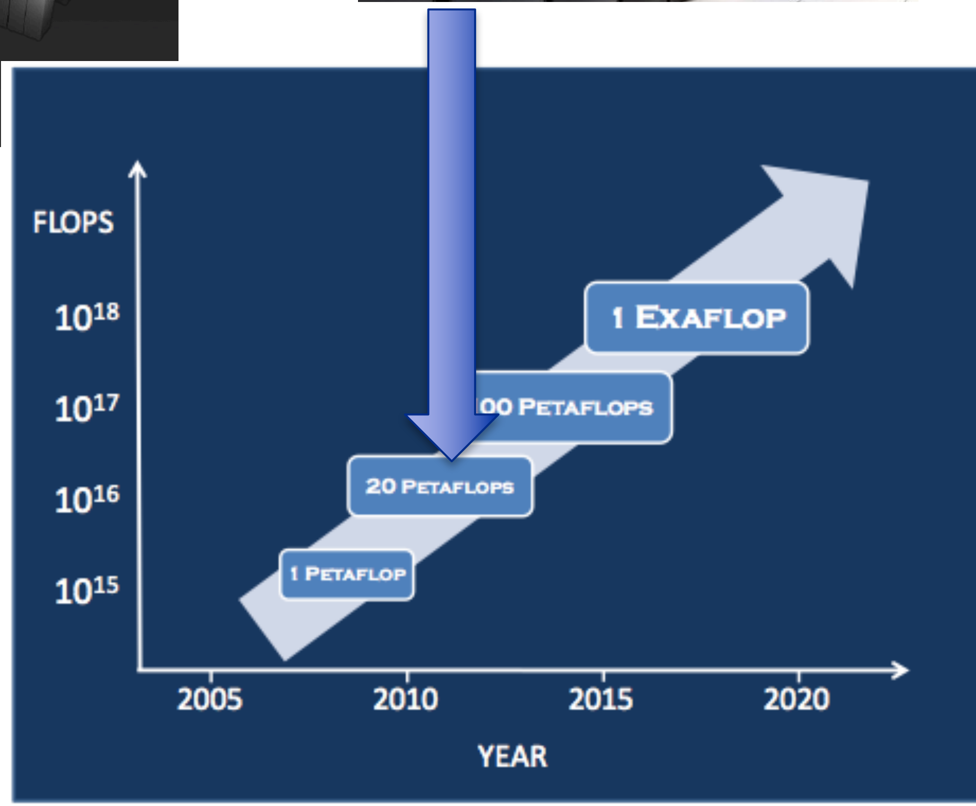

Preparing for the exascale, OLCF, 2009

Motivation – Computation Facilities

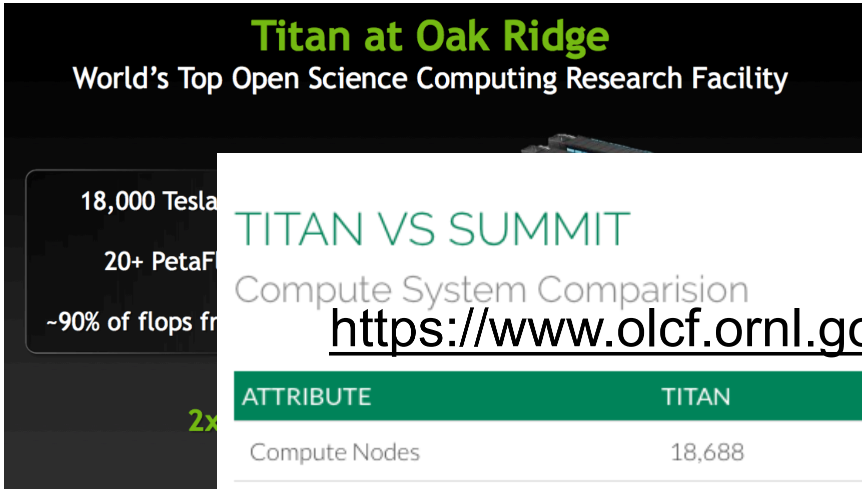

TITAN VS SUMMIT

IBM Mellanox TECHNOLOGIES NVIDIA

Compute System Comparision

https://www.olcf.ornl.gov/summit/

ATTRIBUTE	TITAN	SUMMIT
Compute Nodes	18,688	~3,400
Processor	(1) 16-core AMD Opteron per node	(Multiple) IBM POWER 9s per node
Accelerator	(1) NVIDIA Kepler K20x per node	(Multiple) NVIDIA Volta GPUs per node
Memory per node	32GB (DDR3)	>512GB (HBM+DDR4)
CPU-GPU Interconnect	PCI Gen2	NVLINK (5-12x PCIe3)
System Interconnect	Gemini	Dual Rail EDR-IB (23 GB/s)
Peak Power Consumption	9 MW	10 MW

The Free Lunc
Toward (

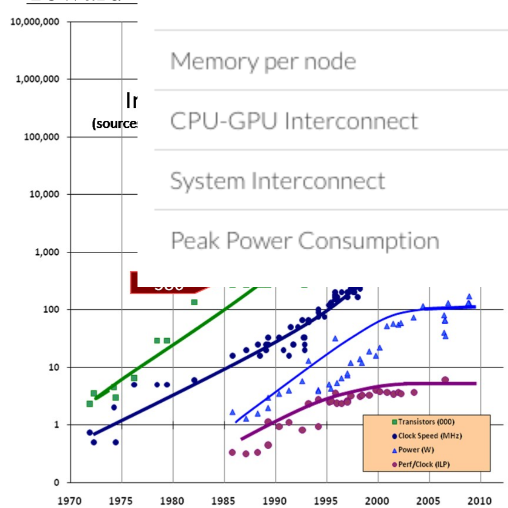

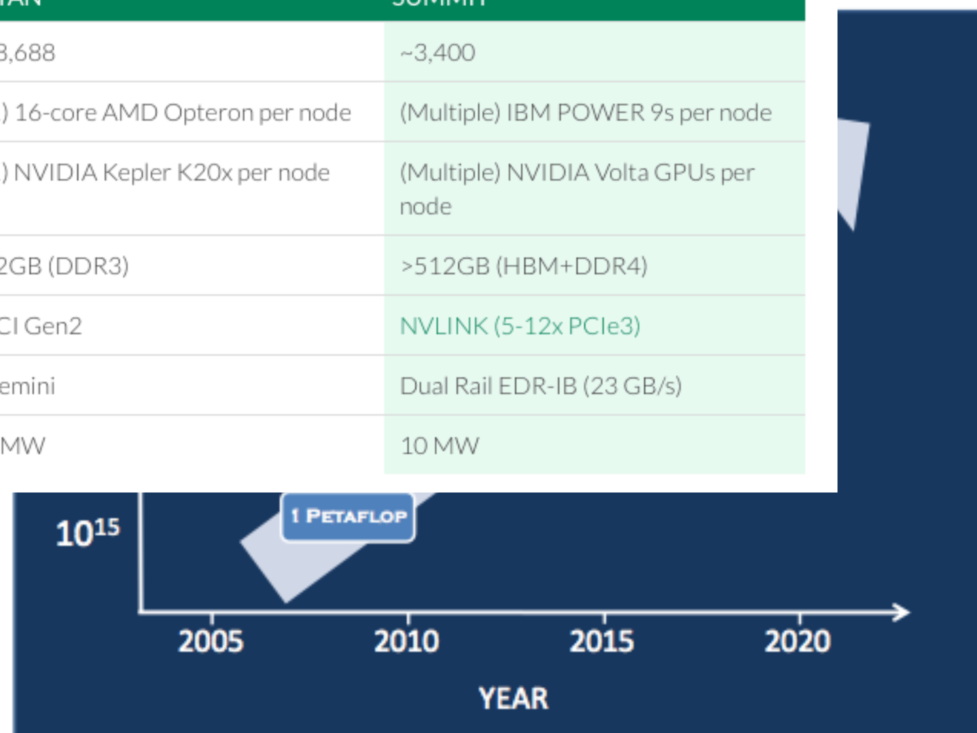

Preparing for the exascale, OLCF, 2009

Motivation – Experimental Facilities

HFIR

One of the highest steady-state neutron flux research reactor in the world

SNS
SPALLATION NEUTRON SOURCE

Spallation Neutron Source

World's most powerful accelerator-based neutron source

Motivation – Why Neutrons

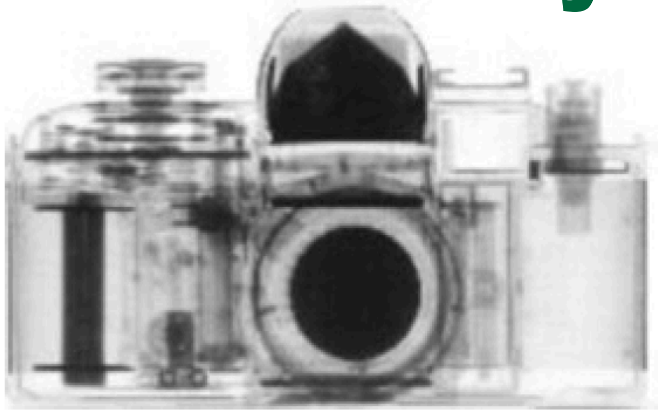

Neutron

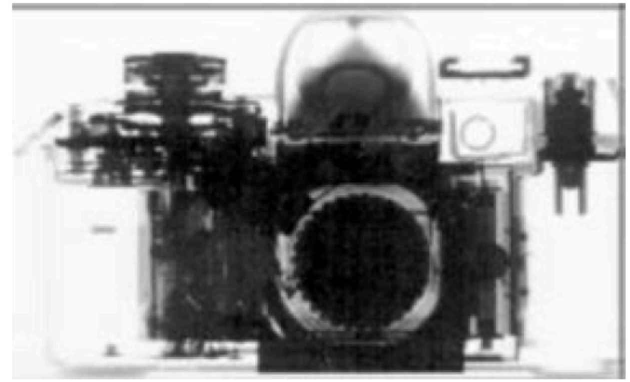

X-ray

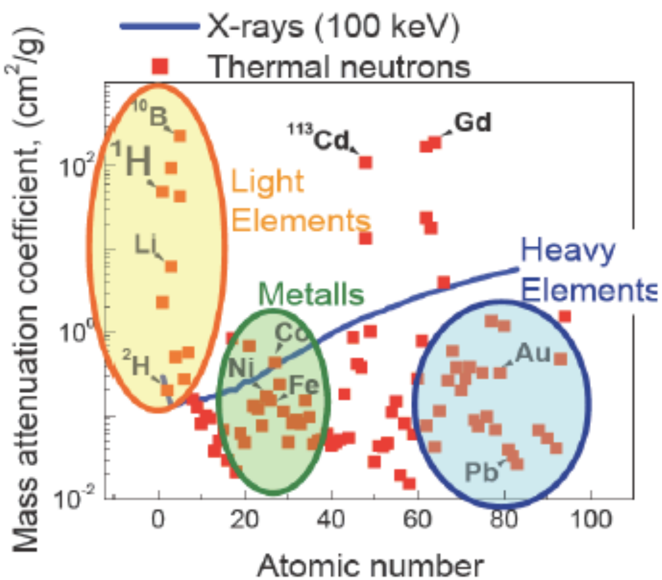

- Penetrate metals without absorbing
- Highly sensitive to water and hydrocarbons
- High contrast to light elements
- Sensitivity to magnetism
- Measure dynamics and structure

Motivation – General Equations

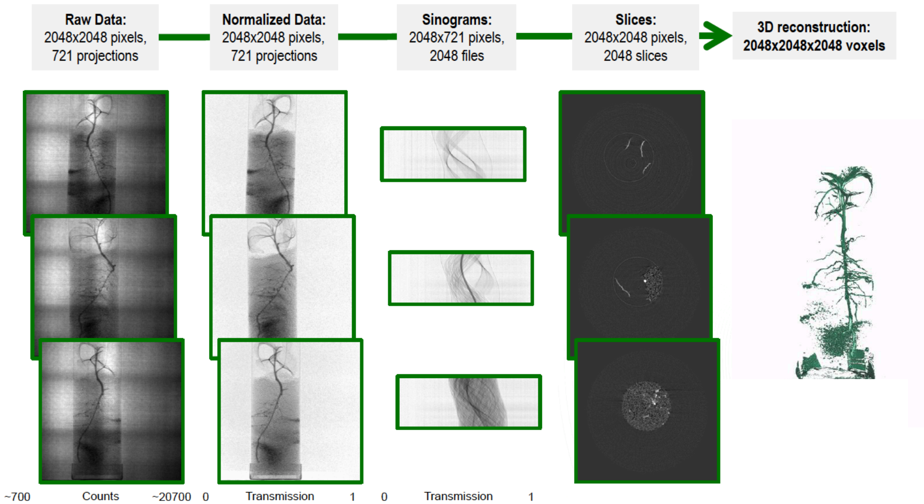

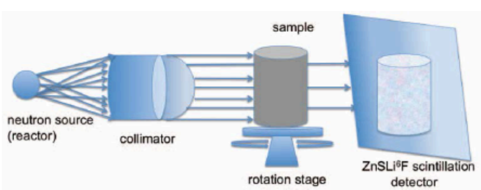

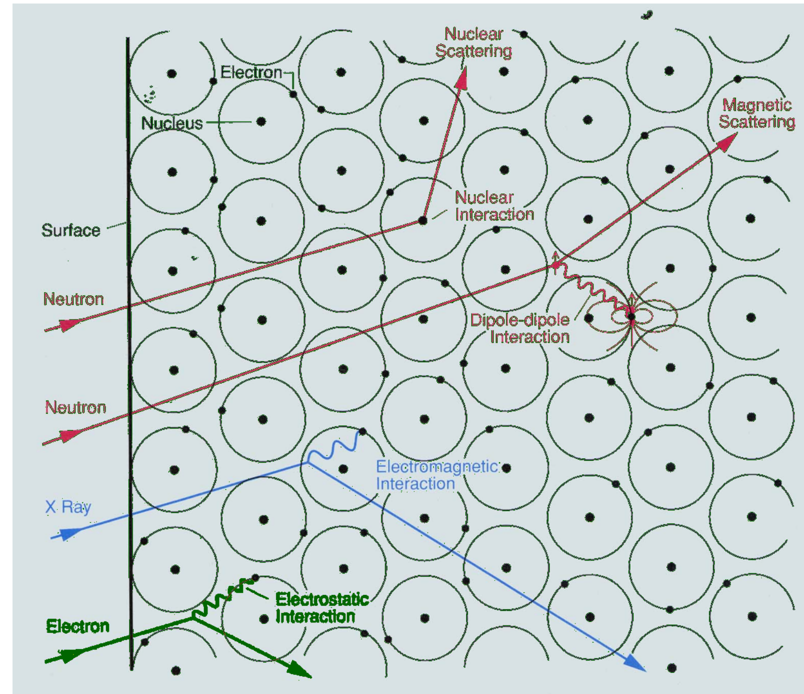

Tomography

$$\mathcal{M} = \int F(u)\delta\Omega$$

Scattering

$$I_{\{\Phi\}}(\mathbf{Q},\omega) = S_{\{\Phi\}}(\mathbf{Q},\omega) * R(\mathbf{Q},\omega)$$

Motivation – Experimental Facilities

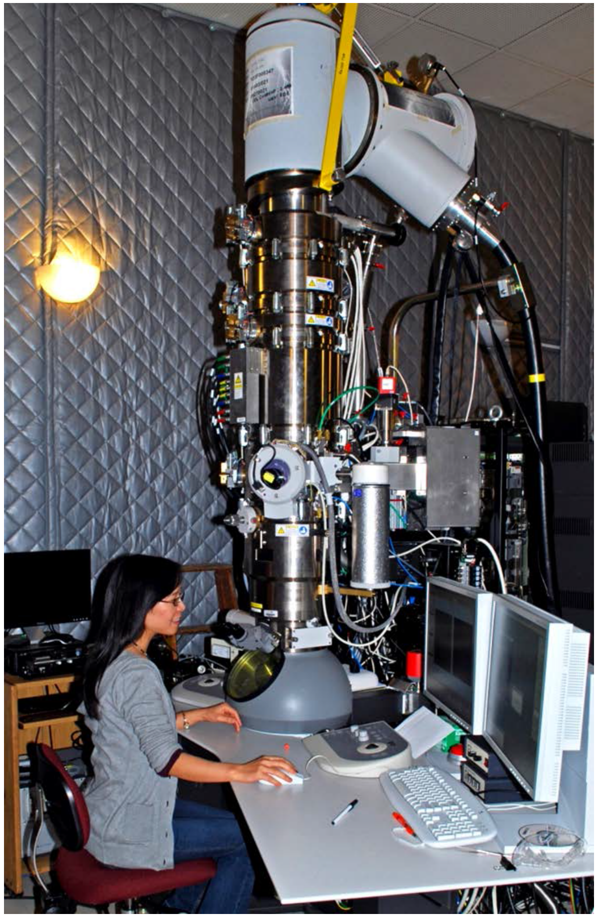

CNMS

Center for Nanophase Materials Sciences

State-of-the-art nanoscience experimental equipment including STEM-TITAN, Atomic Probe, & SPM

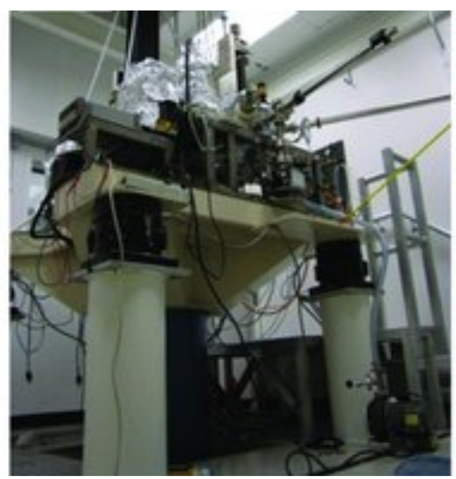

Motivation – Why Electrons

Scanning Transmission Electron Microscopy

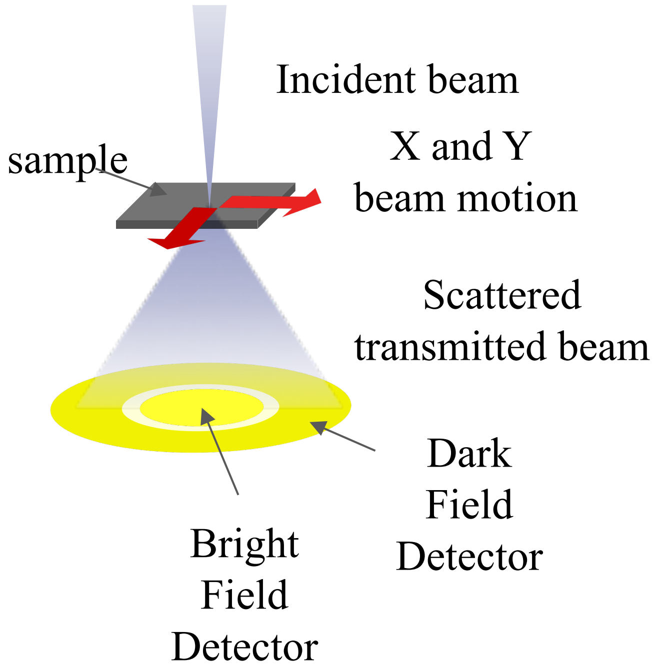

Scanning Probe Microscopy

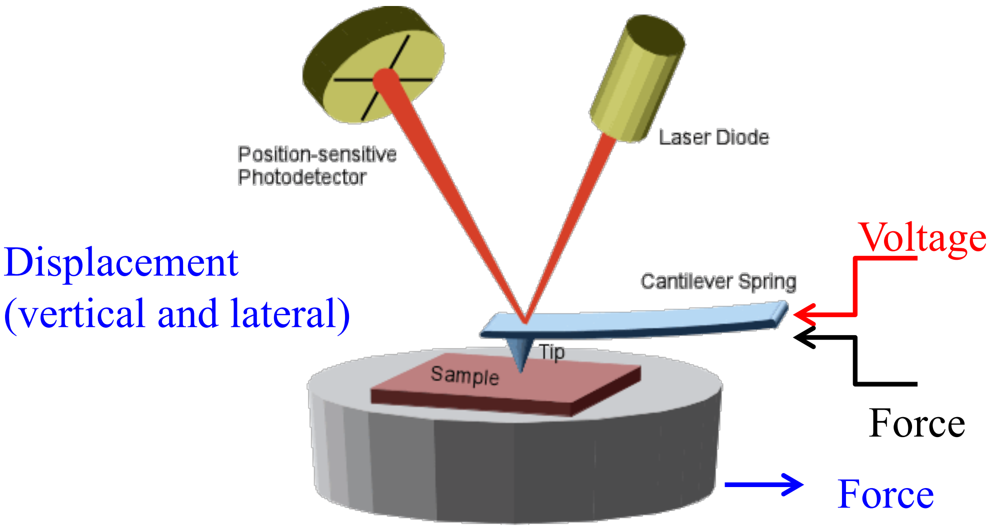

Why Electrons? Understanding of material surface properties.

Atomic resolution of local surface physics and chemistry.

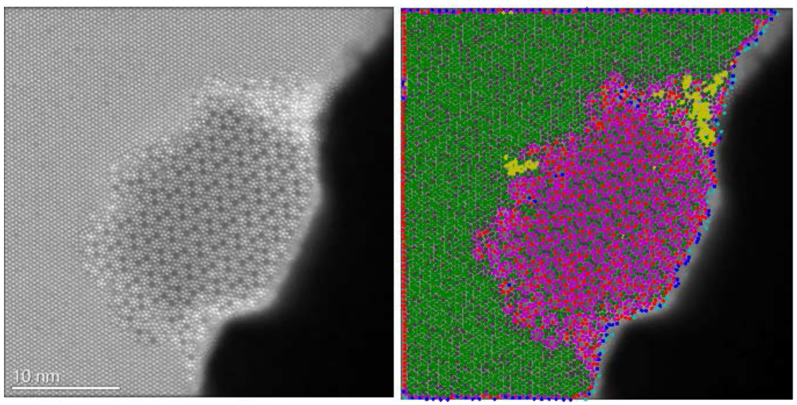

Texture analysis shows Molybdenum–Vanadium based complex oxide catalysts for propane ammoxidation

Q He, J Woo, A Belianinov, VV Guliants, A Borisevich; ACS nano, **DOI:** 10.1021/acsnano.5b00271, (2015)

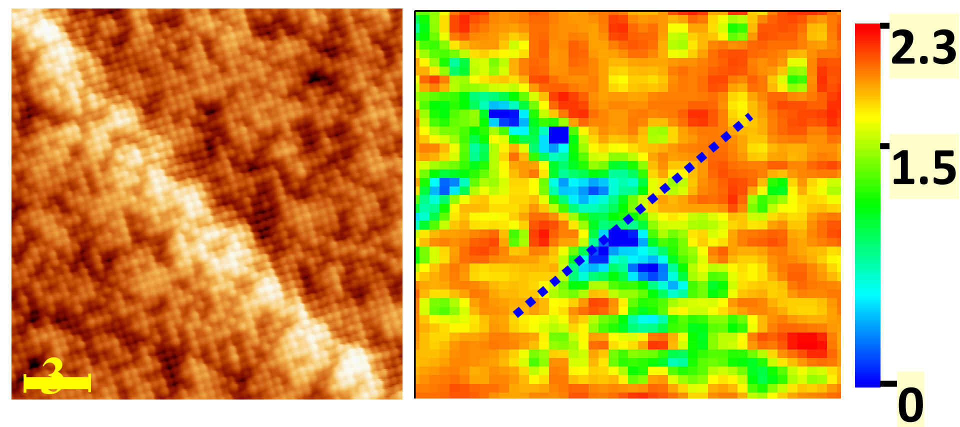

Multivariate analysis shows that superconductivity is suppressed in FeSeTe at the defect

A. Gianfrancesco, A. Belianinov, S. Jesse, and S. Kalinin, Microscopy & Microanalysis, DOI:10.1017/S1431927615012507, (2015)

ACCURATE QUANTIFIED MATHEMATICAL METHODS FOR NEUTRON and EXPERIMENTAL SCIENCE (*ACUMEN*)

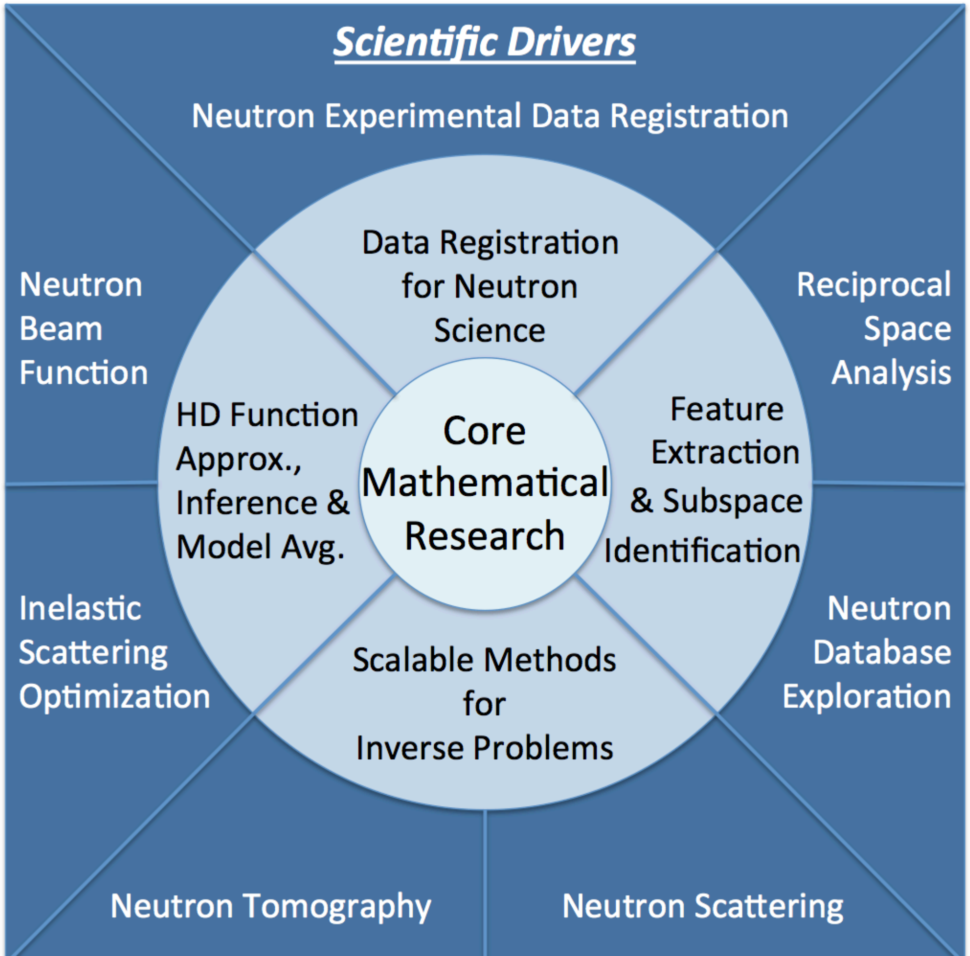

ACUMEN will develop scalable mathematical research that will impact neutron science. Focused targets for first year:

- Neutron Tomography
- Neutron Scattering
- Inelastic Scattering Optimization
- Resolution Function
- Institute involvement and Laboratory investment

ASCR Funded Project under Dr. Steve Lee.

ACUMEN integrates Mathematics with Instruments Scientists

ORNL Facility	Instrument Scientist
CNMS	Dr. Sergei Kalinin *Burton Medal, Microscopy Soc. of America* *Dir. of Inst. Funct. Imaging of Materials*
SNS SPALLATION NEUTRON SOURCE	Dr. Greg Smith *NSSA Fellow* *Structure and Dynamics of Soft Matter GL* Dr. Mark Lumsden *Time-of-Flight Spectroscopy GL* *Mantid Scientific Committee Member* Dr. Anibal Ramirez-Cuesta *Spectroscopy GL* *Instrument Lead for VISION* Dr. Olivier Delaire, 2008-2011 *Clifford G. Shull Fellow,* *DOE Early Career Research Award 2014* Dr. Garrett Granroth *Scientific Data Analysis GL* *Instrument Lead for SEQUOIA*
HFIR	Dr. Hassina Bilheux *Lead for HFIR Beam line CG-1D* *Instrument Lead for future SNS VENUS*

Neutron Tomography

Scientist – H. Bilheux

Mathematicians – R. Archibald & R. Barnard

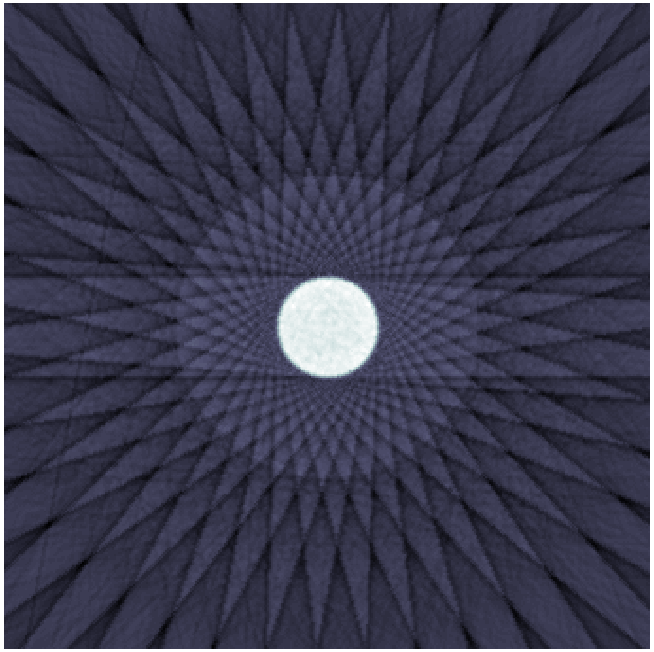

- Standard filtered back projection methods in tomographic reconstruction yields artifacts as seen on the *top left*.
- Image is of Aluminum-Steel Phantom taken at HIFIR - CG1

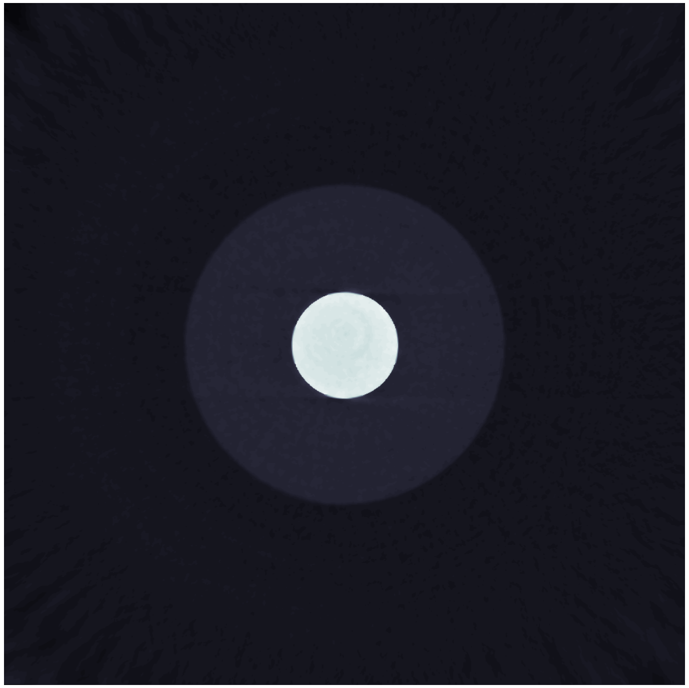

- Scalable high order sparse optimization methods provide fast solutions to tomographic images as seen on the *bottom right*.
- Future VENUS tomography instrument at SNS will produce majority of total data generated at SNS

Inelastic Neutron Scattering

Scientist – Olivier Delaire

Mathematicians – Feng Bao, Ed D'Azvedo & Miro Stoyanov

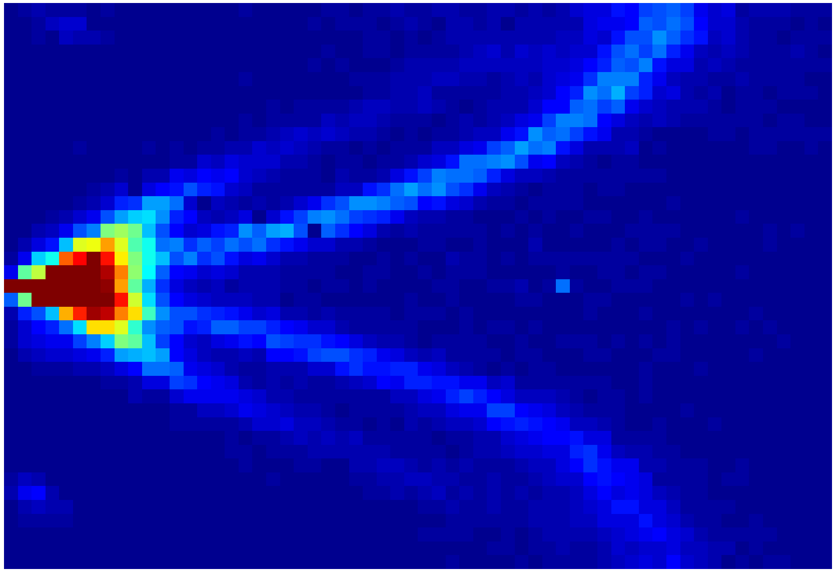

- Time-of-Flight Neutron Spectrometer used to measure Niobium on TOPAZ as seen on the *top right.*
- S(Q,E) space is four dimensional, forming a large search space to optimize.

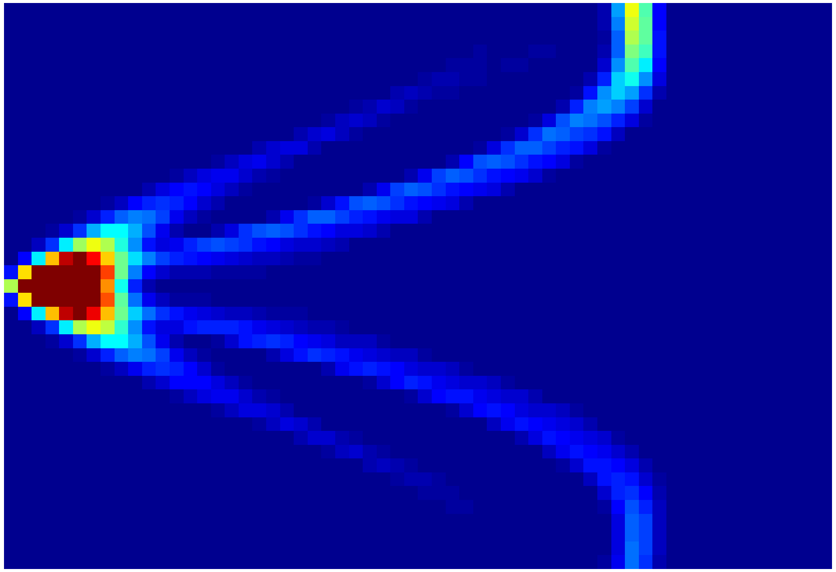

- Theoretical phonon calculation using DFT computationally expensive.
- Developed scalable optimization of DFT with probabilistic bounds of solution.
- Whole S(Q,E) spaced optimized *bottom left.*

VISION Instrument

Scientist – Tim Ramirez-Cuesta

Mathematicians – Guannan Zhang & Clayton Webster

- Working within the mantid software framework for VISION to embed uncertainty quantification algorithms
- Large amounts of information in raw data of scattering events *top right.*

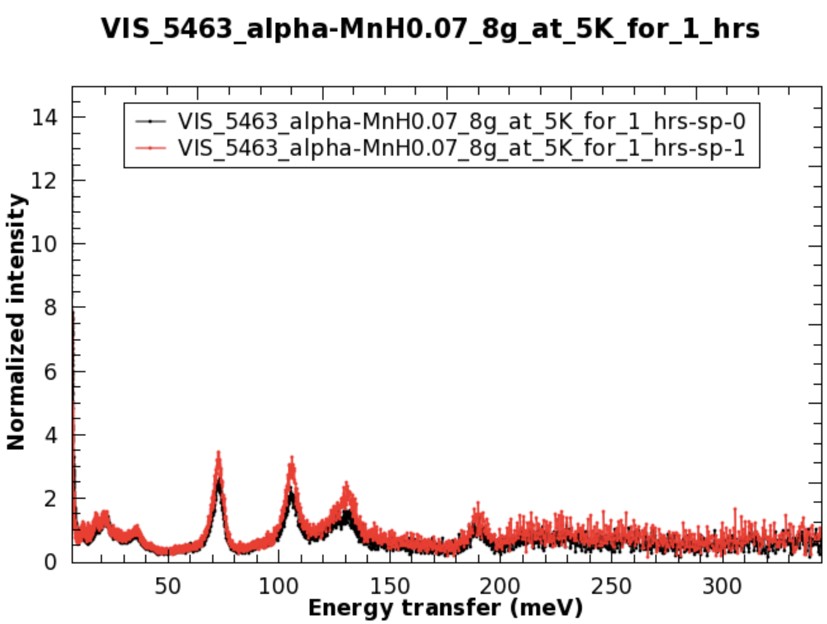

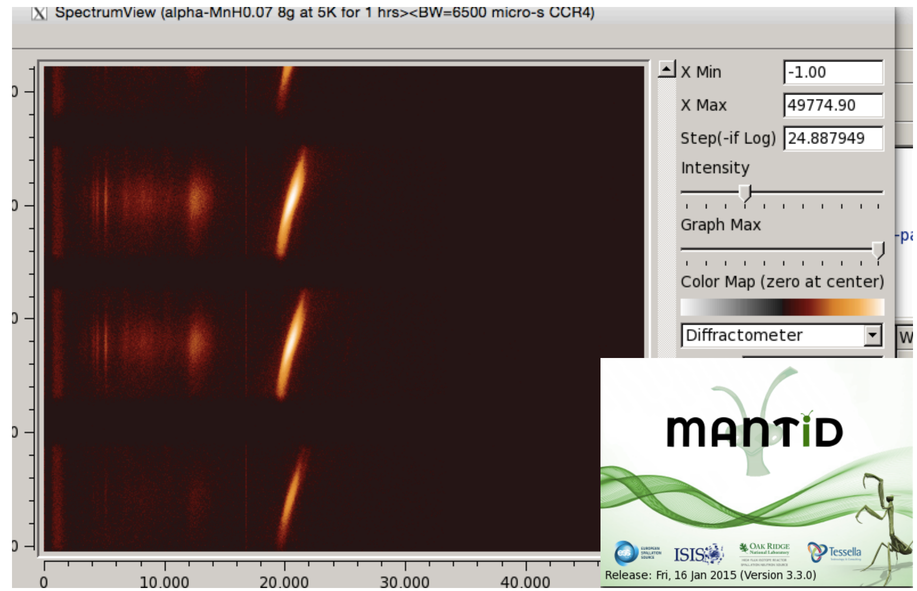

- Resolution at high energies is low for spectrum *bottom left*
- Using Bayesian analysis on the raw data to provide best mean estimate and uncertainty at high energies of spectrum

High Dimensional Resolution Function Estimation

Scientist – Garrett Granroth

Mathematicians – Ed D'Azvedo & Miro Stoyanov

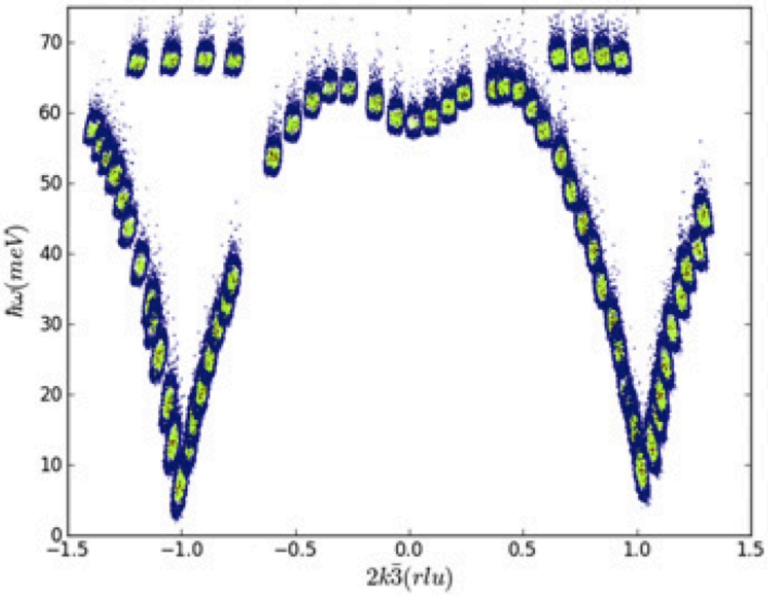

- Need to estimate resolution function is ubiquitous at the DOE experimental facilities
- Often resolution function depends upon many parameters, with different characteristic across parameter space

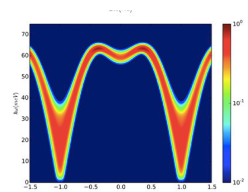

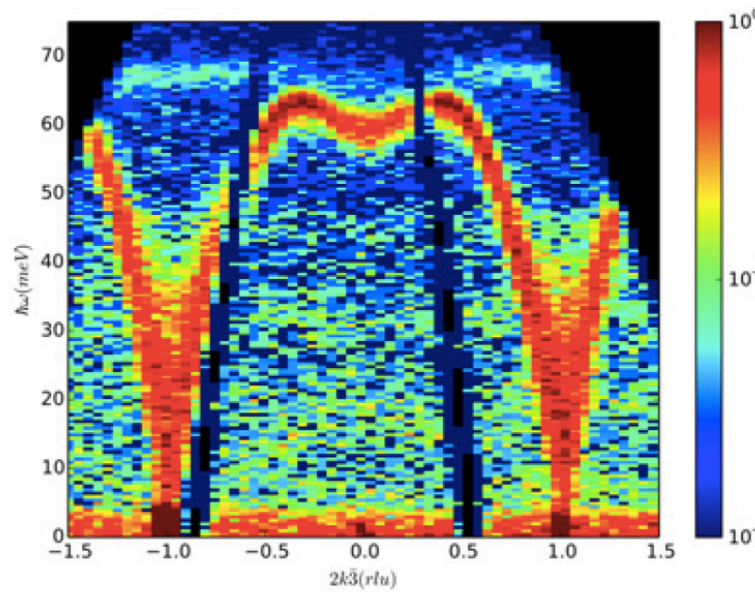

- *McStas (www.mcstas.org)* uses Monte Carlo statistics to simulate resolution function for SEQUOIA
- Building in mathematics from UQ to accelerate resolution function estimation for high dimensional parameter space.

Data Analytics for Microscopy

Scientist – Sergei Kalinin

Mathematicians – Eirik Endeve & Rick Archibald

$SrTiO_3$ substrate

1200 sec.

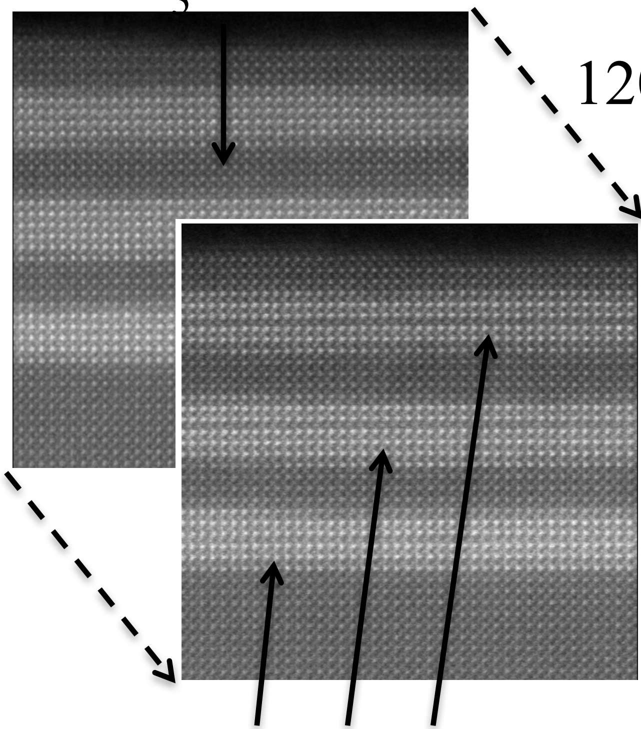

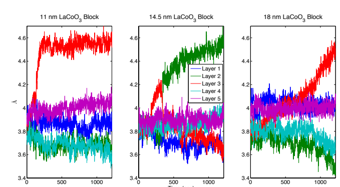

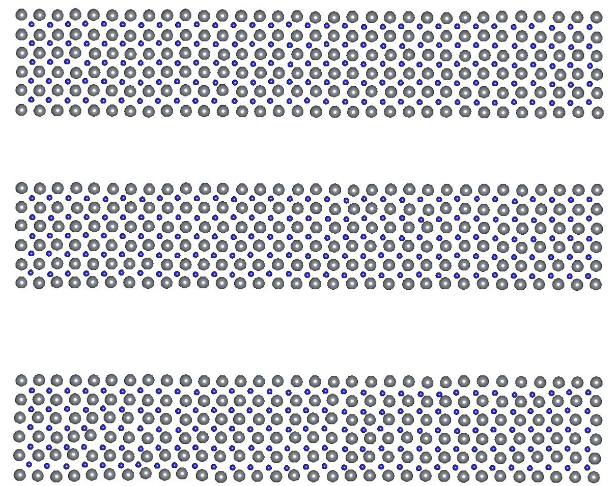

MATERIALS PROJECT

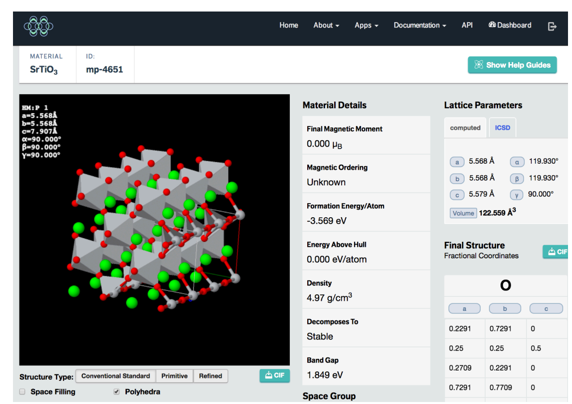

$LaCoO_3$ at 11nm, 14.5nm, & 18nm

Connecting with ORNL Institutes and Infrastructure

Collaboration - Institute for Functional Imaging of Materials

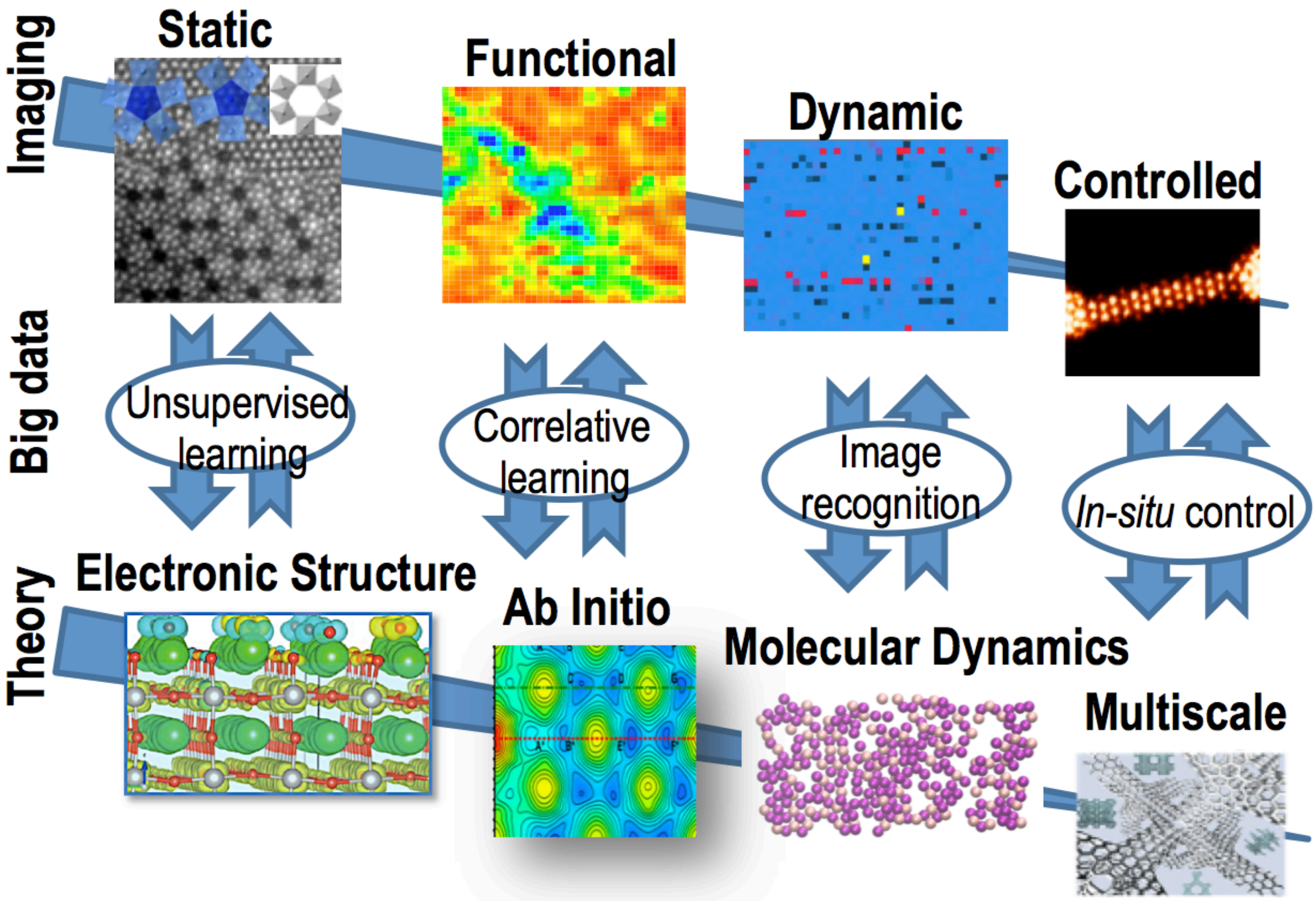

Institute will bridge imaging and theory using HPC data analytics to reveal local physical, chemical and structure-properties in materials, and use this knowledge to enable the design of new materials with tailored functionalities.

Data Analytics for Microscopy

Scientist – Sergei Kalinin

Mathematicians – Eirik Endeve & Rick Archibald

ORNL: STEM/EELS
ANL: Focused X-ray

- High throughput image capture
- Multi-modal:
  -High-angle annular dark field (HAADF) detector
  - Electron energy loss spectroscopy
  - Focused X-ray
- O(1000) of images per experiment

Minutes

Transfer files to HPC storage and convert data to HDF5 format

- Data motion via BBCP/GridFTP
- Data conversion from DM3 stacks to HDF5 slices
- Standard data format (HDF5)
- Data layout conducive to HPC algorithms

Seconds

Massively parallel Image processing/ feature detection

- Denoise Image
- Identify atoms
- Identify lattice
- Thousands of images/sec
- Built on MPI +Fortran
- Near linear scaling – some limitations as file counts get extremely large

Seconds

Massively parallel electronic structure calculation

- Massively parallel study of hundreds to thousands of individual configurations
- Calculation of electronic structure
- Based on DFT
- 0(1000) of configurations

Minutes

Software Integration Strategy

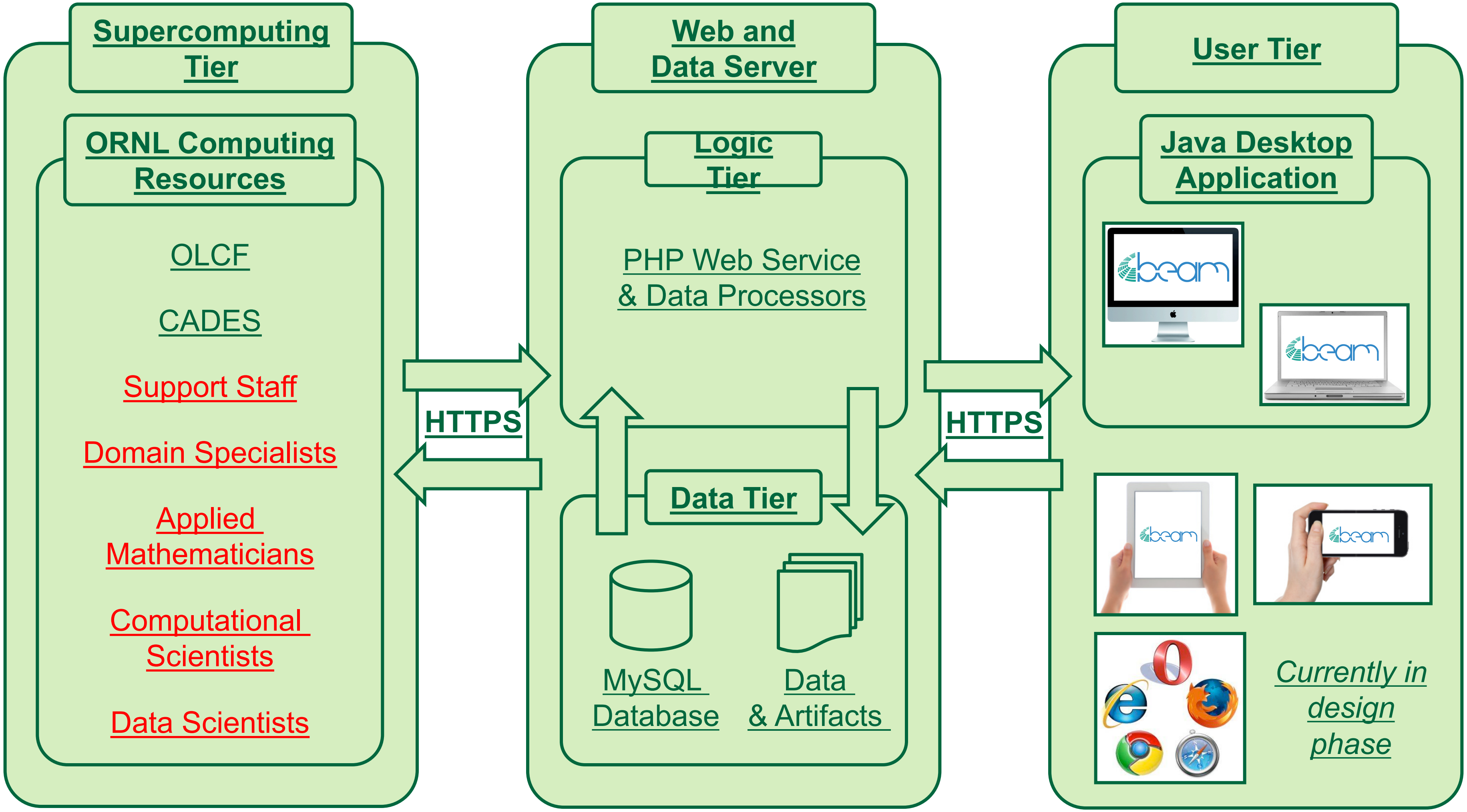

Big Data and High Performance Computing

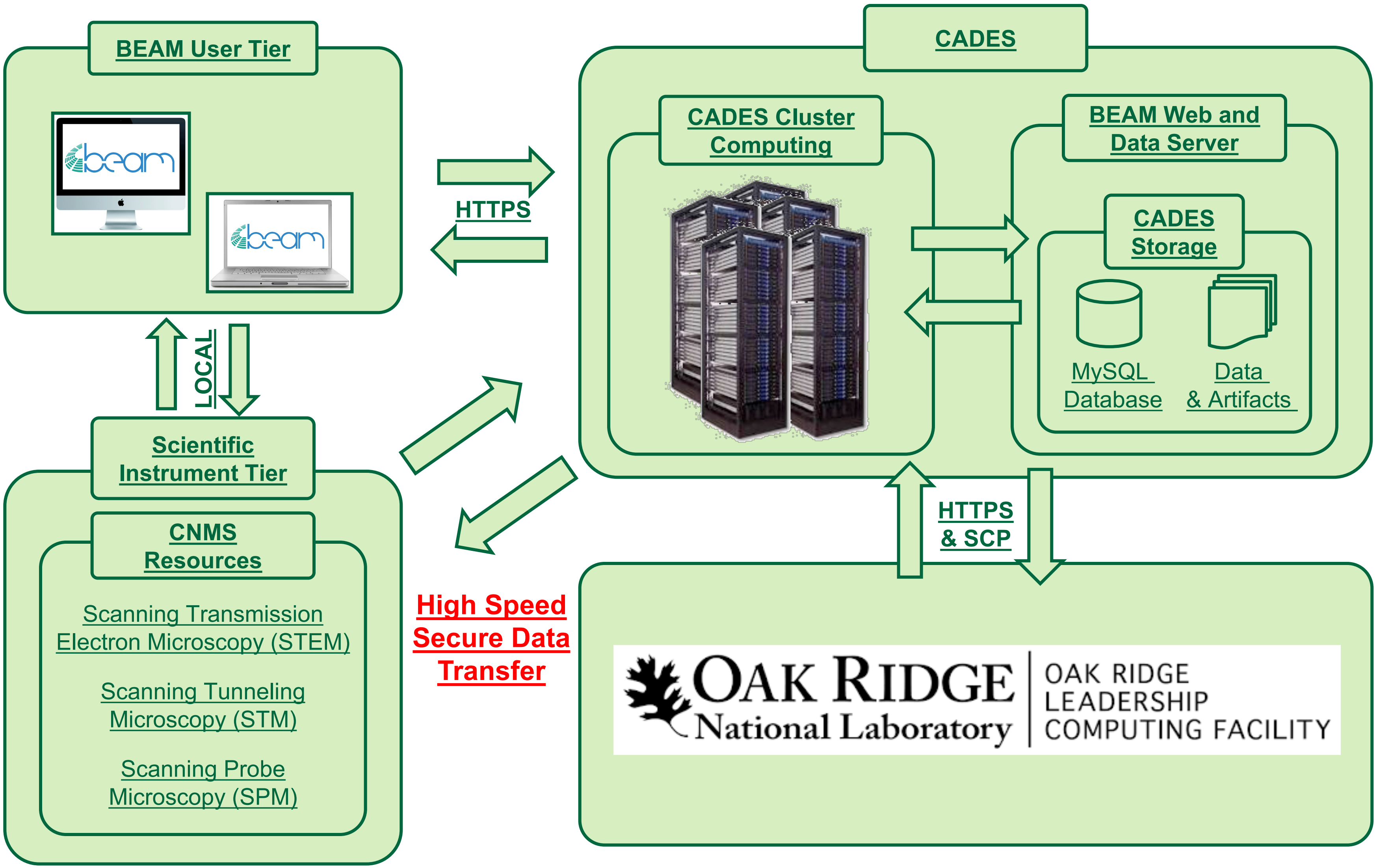

Big Data and High Performance Computing

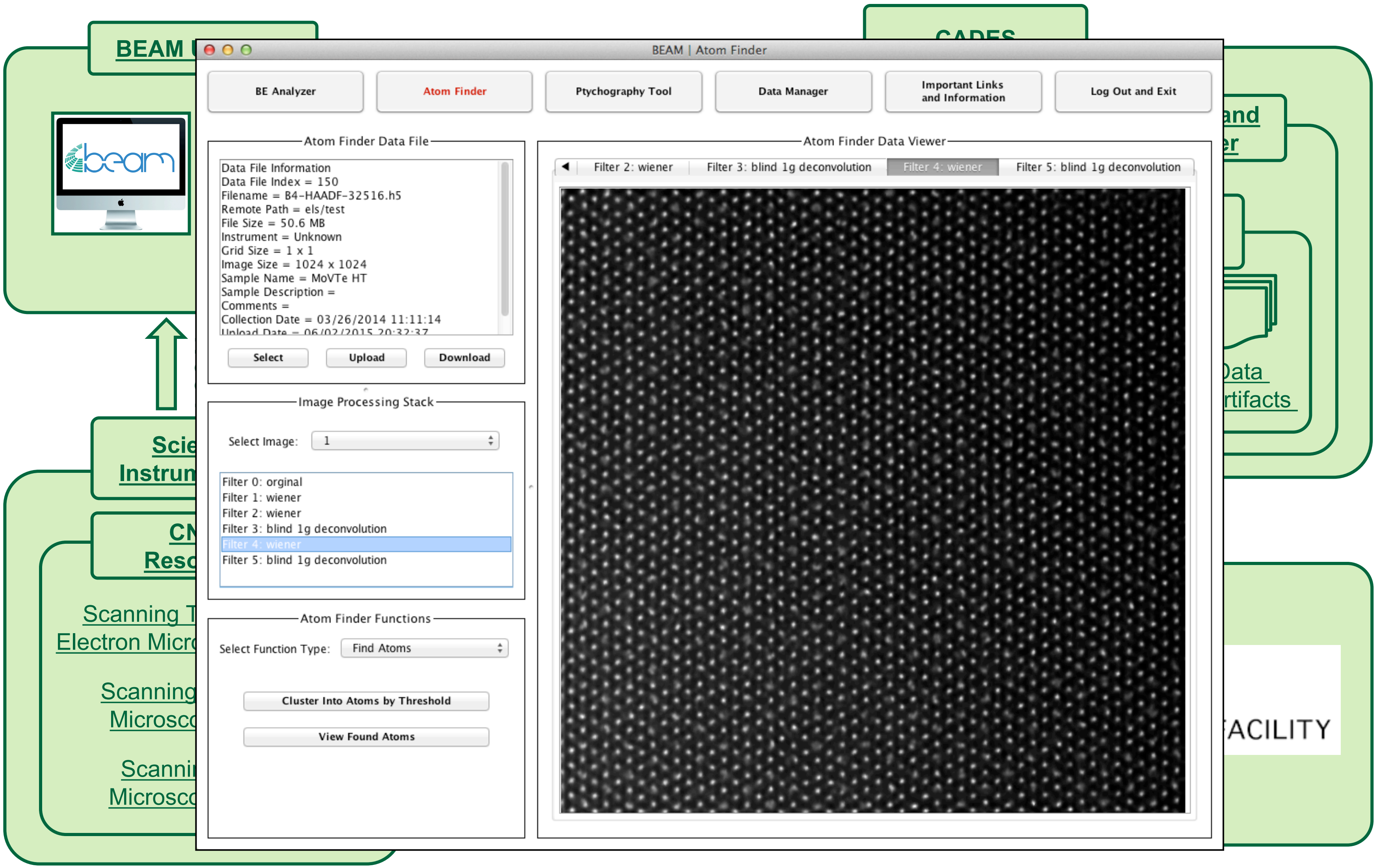

Basic principle of CT
-Reconstruction of 2 dimensional image-

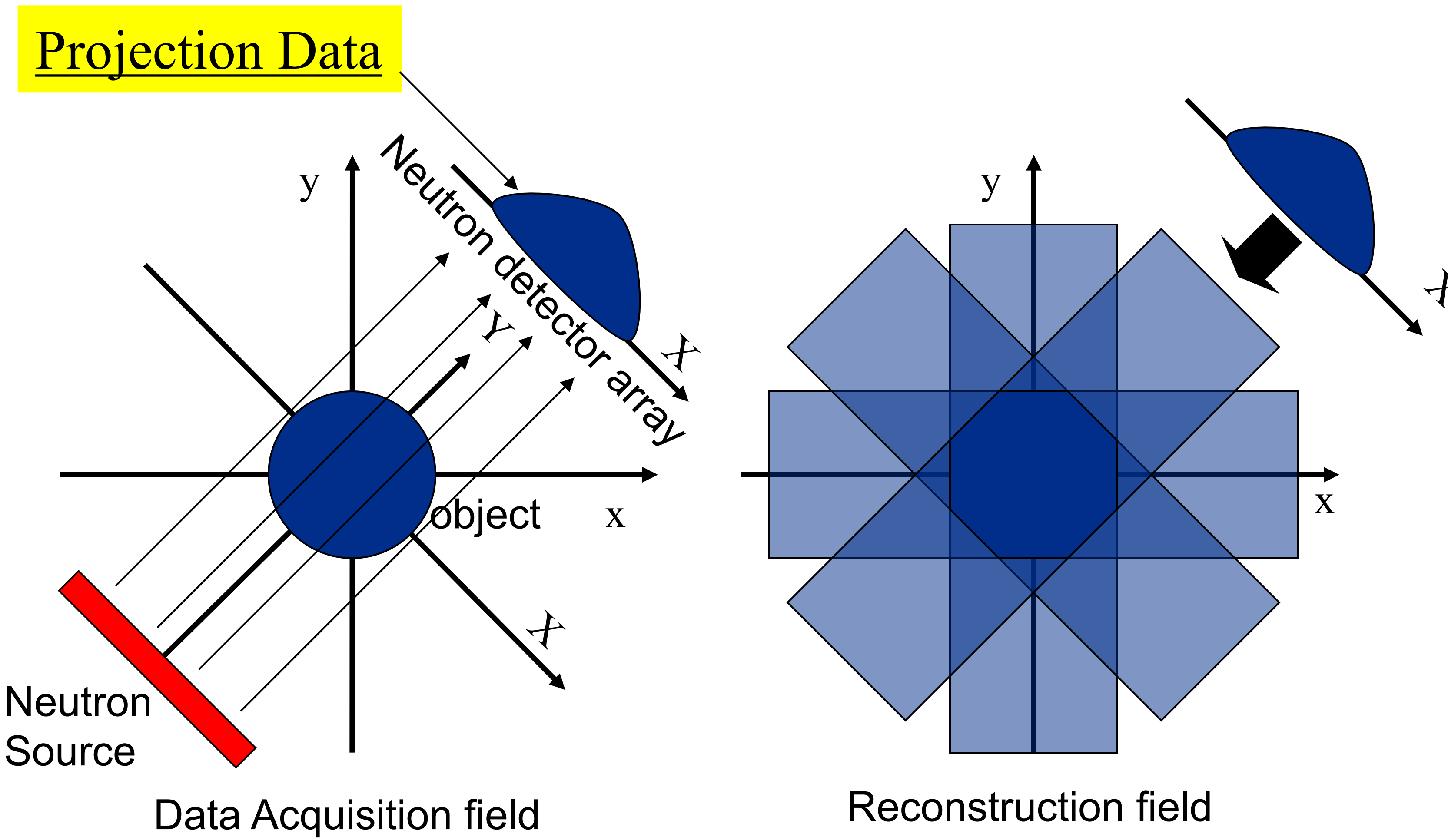

Reconstruction process

$f(x, y)$: absorption coefficient (to be reconstructed) [Np/m]

$I_0(x)$: incident intensity, $I(x)$: attenuated intensity

attenuated intensity : $I(X) = I_0(X)e^{-\int f(x,y)dY}$

projection data : $p(X, \theta) = \int f(x, y)dY = \ln \dfrac{I_0(X)}{I(X)}$

Filtered data : $p_f(X, \theta) = \dfrac{1}{2\pi}\int_{-\infty}^{\infty} P(U, \theta) \cdot |U| \cdot e^{jUX} dX$

where $P(U, \theta)$ is 1D FFT of $p(X, \theta)$

Back projection : $f(x, y) = \int_0^{\pi} p_f(x \cdot \cos\theta + y \cdot \sin\theta, \theta)d\theta$

SL Phantom

True image

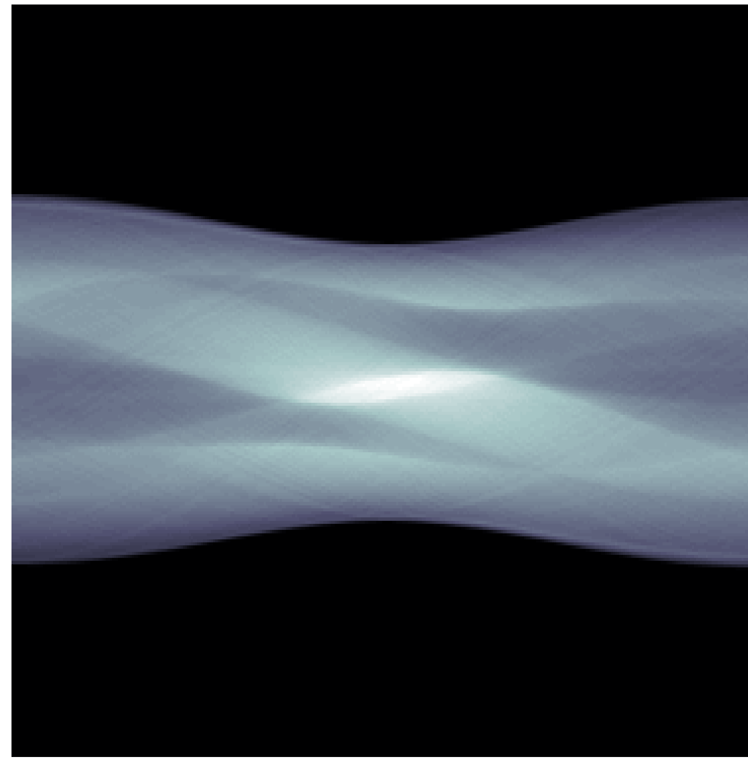

Measured Data
(Sinogram)

SL Phantom

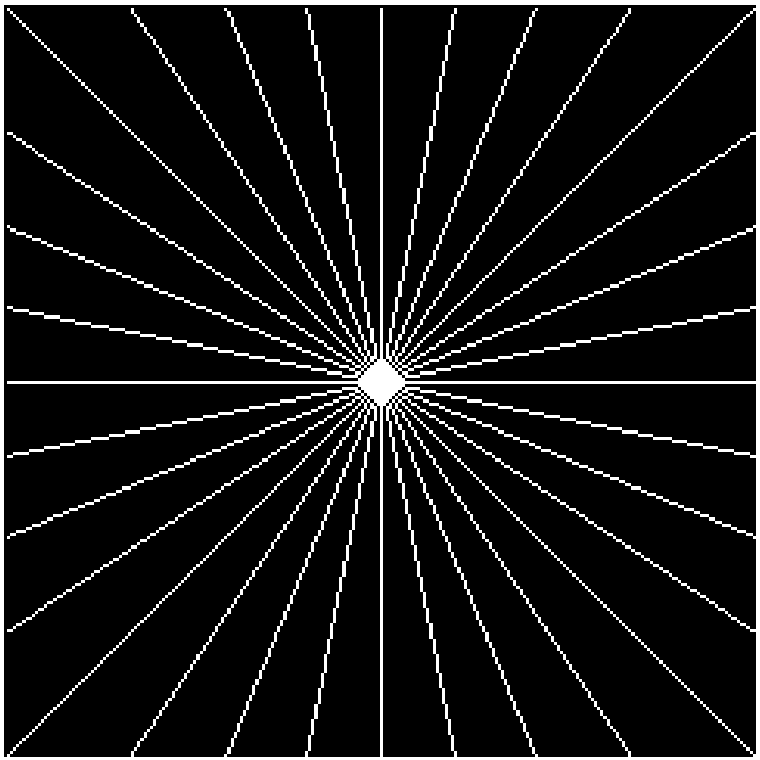

Known Fourier Data

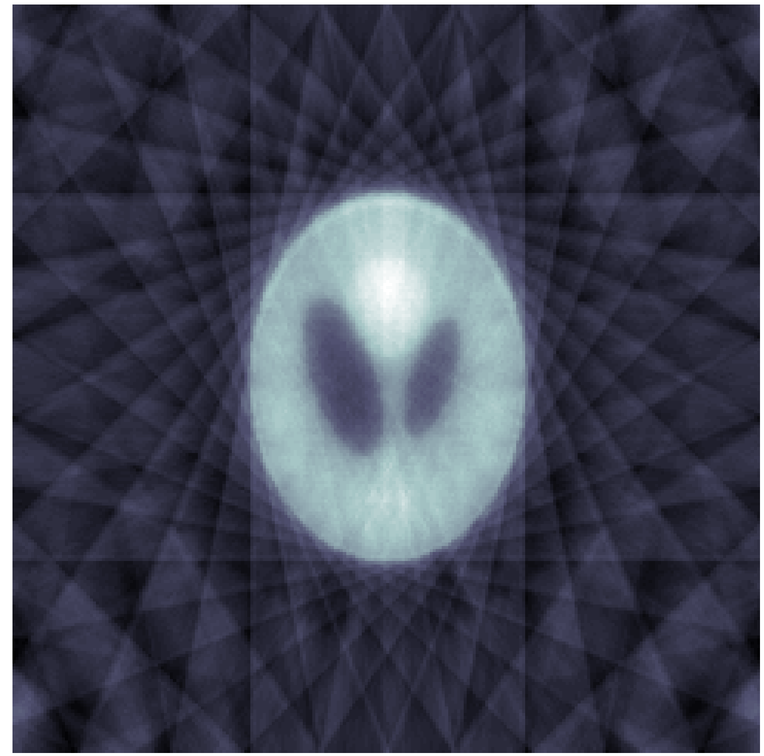

Partial Reconstruction

Partially Sampled Fourier Data

Determine $\mathbf{f} = \{f(x_i, y_j) : 0 \leq i, j \leq 2N\}$ that solves the convex optimization problem

$$\begin{aligned} &\text{minimize} \;\; ||J_x\mathbf{f}||_1 + ||J_y\mathbf{f}||_1, \\ &\text{subject to} \;\; ||MF\mathbf{f} - \hat{\mathbf{f}}||_2 \leq \sigma, \end{aligned}$$

Where the matrix M is a mask that removes unknown Fourier coefficients.

Partially Sampled Fourier Data

Split Bregman iteration solves the optimization problem using a sequence of two unconstrained problems of the form

$$
\begin{aligned}
\mathbf{f}^{k+1} &= \min_{\mathbf{f}} ||J_x \mathbf{f}||_1 + ||J_y \mathbf{f}||_1 + \frac{\mu}{2} ||MF\mathbf{f} - \hat{\mathbf{f}}^k||_2, \\
\hat{\mathbf{f}}^{k+1} &= \hat{\mathbf{f}}^k + \hat{\mathbf{f}} - MF\mathbf{f}^{k+1}
\end{aligned}
$$

for optimization parameter $\mu > 0$.

Goldstein, T., and Osher, S. The split bregman method for l1-regularized problems. SIAM Journal on Imaging Sciences 2, 2 (2009), 323–343.

Partially Sampled Fourier Data

Using the total variation operator ($J_x = \nabla_x$ and $J_y = \nabla_y$), with the replacements, $\mathbf{d}_x \leftarrow \nabla_x \mathbf{f}$ and $\mathbf{d}_y \leftarrow \nabla_y \mathbf{f}$, using $||\nabla \mathbf{v}||_1 = \sum_{i,j} \sqrt{|\nabla_x v_{i,j}|^2 + |\nabla_y v_{i,j}|^2}$, the augmented problem is,

$$\begin{aligned}\min_{\mathbf{f},\mathbf{d}_x,\mathbf{d}_y} \sum_{i,j} \sqrt{|d_{x,i,j}|^2 + |d_{y,i,j}|^2} \quad &+ \quad \frac{\lambda}{2}||\mathbf{d}_x - \nabla_x \mathbf{f} - \mathbf{b}_x||_2 \\ &+ \quad \frac{\lambda}{2}||\mathbf{d}_y - \nabla_y \mathbf{f} - \mathbf{b}_y||_2 + \frac{\mu}{2}||MF\mathbf{f} - \hat{\mathbf{f}}||_2.\end{aligned}$$

This augmented problem is done in steps. When $\mathbf{f}$ is held fixed, the exact optimization of $\mathbf{d}_x$ and $\mathbf{d}_y$ can be calculated by,

$$\mathbf{d}_x^{opt} = \max(\mathbf{s} - 1/\lambda, 0)\frac{\nabla_x \mathbf{f} + \mathbf{b}_x}{\mathbf{s}} \quad \text{and} \quad \mathbf{d}_y^{opt} = \max(\mathbf{s} - 1/\lambda, 0)\frac{\nabla_y \mathbf{f} + \mathbf{b}_y}{\mathbf{s}}, \quad (1)$$

where

$$\mathbf{s} = \sqrt{|\nabla_x \mathbf{f} + \mathbf{b}_x|^2 + |\nabla_y \mathbf{f} + \mathbf{b}_y|^2}.$$

Partially Sampled Fourier Data

When $\mathbf{d}_x$ and $\mathbf{d}_y$ are held fixed the l^2 problem

$$\min_{\mathbf{f}} \frac{\lambda}{2}||\mathbf{d}_x - \nabla_x \mathbf{f} - \mathbf{b}_x||_2 \frac{\lambda}{2}||\mathbf{d}_y - \nabla_y \mathbf{f} - \mathbf{b}_y||_2 + \frac{\mu}{2}||MF\mathbf{f} - \hat{\mathbf{f}}||_2.$$

Because this subproblem is differentiable, we can find the optimal solution $\mathbf{f}$ by differentiating by $\mathbf{f}$ and setting the result equal to zero to get,

$$(\mu F^T M^T M F + \lambda \nabla_x^T \nabla_x + \lambda \nabla_y^T \nabla_y)\mathbf{f} = rhs,$$

where

$$rhs = \mu F^T M^T \hat{\mathbf{f}} + \lambda \nabla_x^T(\mathbf{d}_x - \mathbf{b}_x) + \lambda \nabla_y^T(\mathbf{d}_y - \mathbf{b}_y).$$

Partially Sampled Fourier Data

Algorithm: Split Bregmen Optimization of partially sampled Fourier data for the TV operator.

Initialize: $\mathbf{f}^0 = F^{-1}M^T\hat{\mathbf{f}}$, and $\mathbf{b}_x = \mathbf{b}_y = \mathbf{d}_x = \mathbf{d}_y = k = 0$

while $||MF\mathbf{f}^k - \hat{\mathbf{f}}||_2 > \sigma$

$$\mathbf{f}^{k+1} = F^{-1}K^{-1}Frhs^k$$

$$\mathbf{d}_x^{k+1} = \max(\mathbf{s}^k - 1/\lambda, 0)\frac{\nabla_x\mathbf{f}^k+\mathbf{b}_x^k}{\mathbf{s}^k}$$

$$\mathbf{d}_y^{k+1} = \max(\mathbf{s}^k - 1/\lambda, 0)\frac{\nabla_y\mathbf{f}^k+\mathbf{b}_y^k}{\mathbf{s}^k}$$

$$\mathbf{b}_x^{k+1} = \mathbf{b}_x^{k+1} + (\nabla_x\mathbf{f}^{k+1} - \mathbf{d}_x^{k+1})$$

$$\mathbf{b}_y^{k+1} = \mathbf{b}_y^{k+1} + (\nabla_y\mathbf{f}^{k+1} - \mathbf{d}_y^{k+1})$$

$$\hat{\mathbf{f}}^{k+1} = \hat{\mathbf{f}}^k + \hat{\mathbf{f}} - MF\mathbf{f}^{k+1}$$

$$k = k + 1$$

end

Partially Sampled Fourier Data

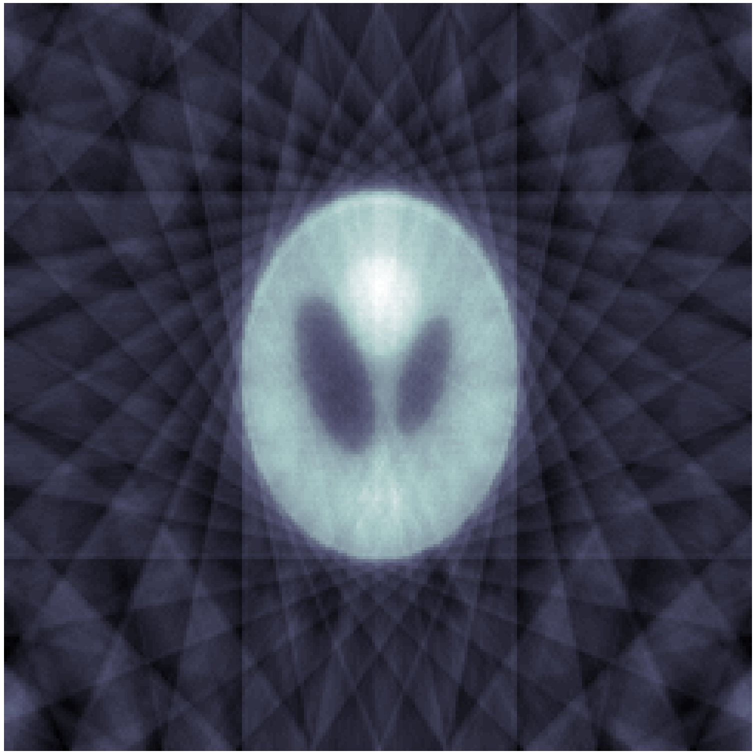

Partial Reconstruction

Optimized Reconstruction

Multi-Dimensional Formulation

- Let $\mathcal{S}$ be a set of discrete points in the bounded domain $\Omega \subset \mathbb{R}^d$ and f be a piecewise smooth function known only on $\mathcal{S}$.

- We construct a function, $L_N f$ for $N \in \mathbb{N}$, that has the asymptotical convergence property,

$$L_N f(x) \longrightarrow 0,$$

away from jump discontinuities of f.

Multi-Dimensional Formulation

- For any $x \in \Omega$, we choose a set

$$\mathcal{S}_x := \mathcal{S}_{x,N} := \{x_1, \ldots, x_N\},$$

which is a local set typically of $N = m_d := \binom{m+d}{d}$ points around x.

The edge detection method is based on a local polynomial annihilation property and performed in the following two steps:

1. Solve the linear system

$$\sum_{x_j \in \mathcal{S}_x} c_j(x) p_i(x_j) = \sum_{|\alpha|_1 = m} p_i^{(\alpha)}(x), \quad \alpha \in \mathbb{Z}_+^d,$$

   where p_i, $i = 1, \cdots, m_d$, is a basis of Π_m. Here Π_m denotes the space of all polynomials of degree $\leq m$ in $d \in \mathbb{N}$ variables. Note the dimension of Π_m is $m_d := \binom{m+d}{d}$, and therefore the solution exists and is unique.

2. Our edge detector $L_m f$ is defined as

$$L_m f(x) = \frac{1}{q_{m,d}(x)} \sum_{x_j \in \mathcal{S}_x} c_j(x) f(x_j).$$

   Here $q_{m,d}(x)$ is a suitable normalization factor depending on m, the dimension d, and the local set $\mathcal{S}_x$.

One Dimension

- Let f be a piecewise smooth function known only on the set

$$\mathcal{S} := \{x_j \mid a \leq x_1 < x_2 < \cdots < x_N \leq b\} \subset \mathbb{R}.$$

- Define the local jump function corresponding to f as

$$[f](x) := f(x+) - f(x-),$$

where $f(x+)$ and $f(x-)$ are the right and left side limits of the function f at x.

- Finally define

$$h(x) := \max\{|x_j - x_{j-1}| \; : \; x_{j-1}, x_j \in \mathcal{S}_x\},$$

$$\mathcal{S}_x^+ := \{x_j \in \mathcal{S}_x | x_j \geq x\}, \quad \text{and} \quad \mathcal{S}_x^- := \{x_j \in \mathcal{S}_x | x_j < x\}.$$

The edge detection method is performed in the following two steps:

1. Solve the linear system

$$\sum_{x_j \in \mathcal{S}_x} c_j(x) p_i(x_j) = p_i^{(m)}(x), \quad i = 1, \cdots, m_1,$$

   where p_i, $i = 1, \cdots, m_1$, is a basis of Π_m. Clearly, the coefficients $c_j(x)$ are uniquely determined by the local set $\mathcal{S}_x$, and are of order $\mathcal{O}(h(x)^{-m})$ as $h(x)$ tends to 0.

2. The edge detection method in the one dimensional case is

$$L_m f(x) = \frac{1}{q_m(x)} \sum_{x_j \in \mathcal{S}_x} c_j(x) f(x_j),$$

   where the normalization factor is set as

$$q_m(x) := q_{m,1}(x) := \sum_{x_j \in \mathcal{S}_x^+} c_j(x).$$

To further illustrate the linear system consider the following example:

For $m \in \mathbb{Z}_+$, consider the following basis of Π_m:

$$p_i(x) = x^{i-1} \quad \textit{for } i = 1, \cdots, m_1.$$

It follows that becomes

$$\sum_{x_j \in \mathcal{S}_x} c_j(x) x_j^{i-1} = m! \delta_{i,m_1} \quad \textit{for } i = 1, \cdots, m_1.$$

Specifically, let $m = 2$ and $\mathcal{S}_x = \{x_1, x_2, x_3\}$. The linear system can be written in matrix notation as,

$$\begin{pmatrix} 1 & 1 & 1 \\ x_1 & x_2 & x_3 \\ x_1^2 & x_2^2 & x_3^2 \end{pmatrix} \begin{pmatrix} c_1 \\ c_2 \\ c_3 \end{pmatrix} = \begin{pmatrix} 0 \\ 0 \\ 2 \end{pmatrix}.$$

Example - 1D Edge Detection

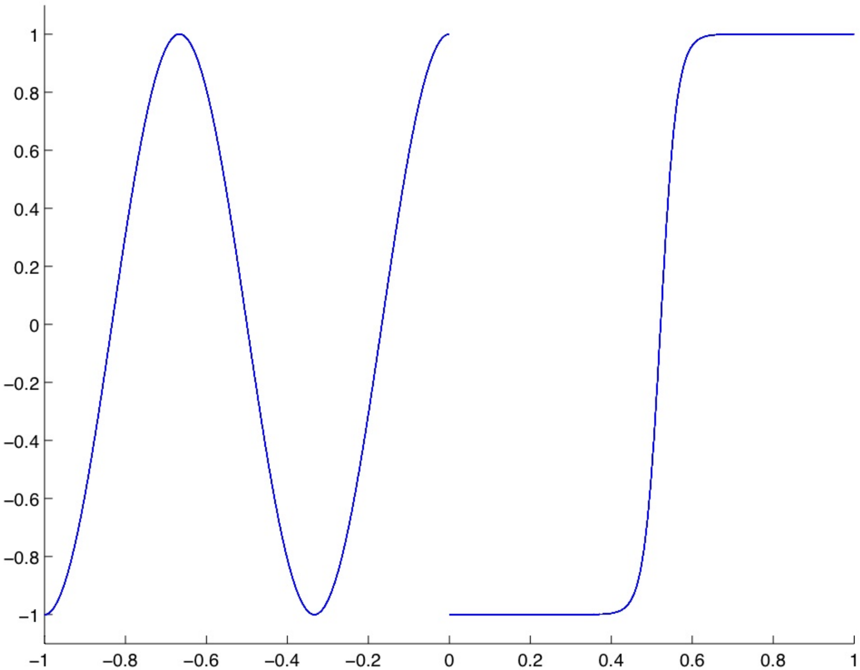

Function

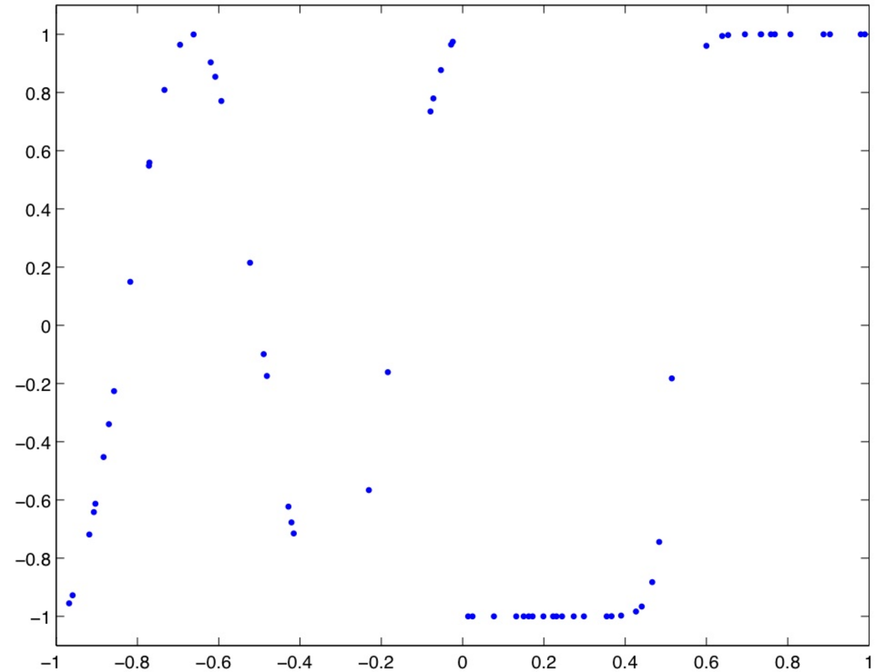

Sampling ($N = 64$)

$$f(y) := \begin{cases} \cos(3\pi y) & -1 \leq y < 0, \\ \frac{2}{1+3e^{-50y+25}} - 1 & 0 < y \leq 1. \end{cases}$$

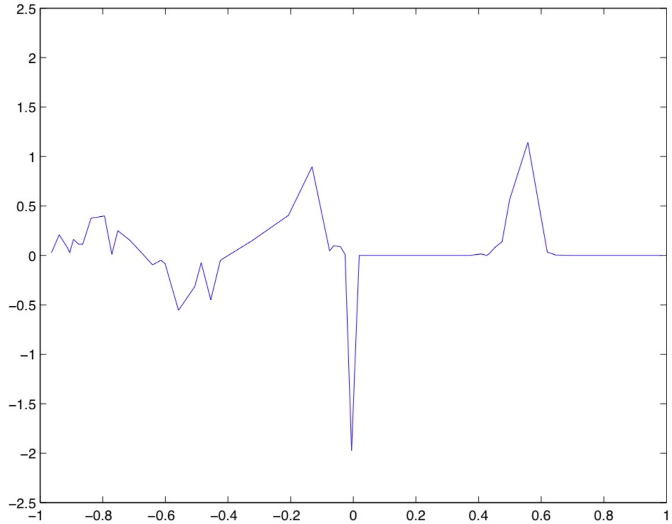

$$L_1 f(y)$$

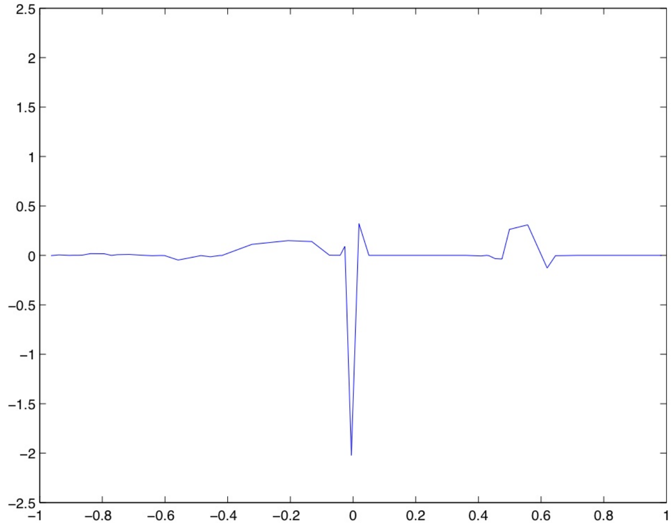

$$L_3 f(y)$$

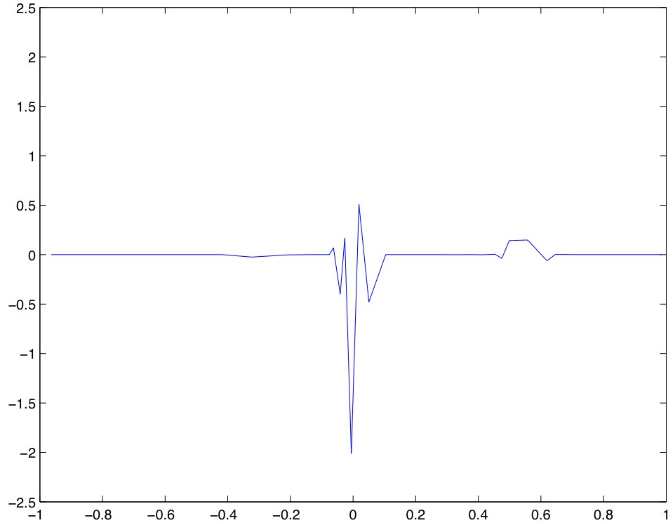

$$L_6 f(y)$$

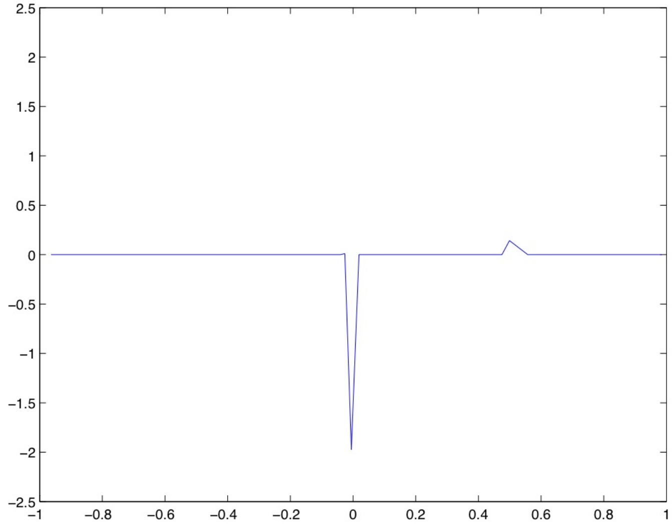

$$MM\Big(L_{\mathcal{M}} f(y)\Big)$$

Partially Sampled Fourier Data

Algorithm: Split Bregmen Optimization of partially sampled Fourier data for the polynomial annihilation operator.

Initialize: $\mathbf{f}^0 = F^{-1}M^T\hat{\mathbf{f}}$, and $\mathbf{b}_x = \mathbf{b}_y = \mathbf{d}_x = \mathbf{d}_y = k = 0$

while $||MF\mathbf{f}^k - \hat{\mathbf{f}}||_2 > \sigma$

$$\mathbf{f}^{k+1} = F^{-1}K_{LM}^{-1}Frhs^k$$

$$\mathbf{d}_x^{k+1} = \max(\mathbf{s}^k - 1/\lambda, 0)\frac{L_{m,x}\mathbf{f}^k + \mathbf{b}_x^k}{\mathbf{s}^k}$$

$$\mathbf{d}_y^{k+1} = \max(\mathbf{s}^k - 1/\lambda, 0)\frac{L_{m,y}\mathbf{f}^k + \mathbf{b}_y^k}{\mathbf{s}^k}$$

$$\mathbf{b}_x^{k+1} = \mathbf{b}_x^{k+1} + (L_{m,x}\mathbf{f}^{k+1} - \mathbf{d}_x^{k+1})$$

$$\mathbf{b}_y^{k+1} = \mathbf{b}_y^{k+1} + (L_{m,y}\mathbf{f}^{k+1} - \mathbf{d}_y^{k+1})$$

$$\hat{\mathbf{f}}^{k+1} = \hat{\mathbf{f}}^k + \hat{\mathbf{f}} - MF\mathbf{f}^{k+1}$$

$$k = k + 1$$

end

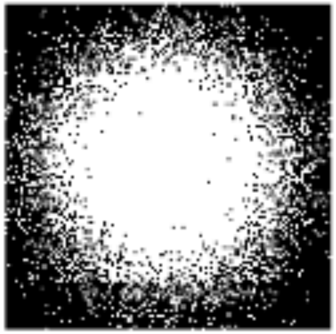

(a) Sampling of 50% of the Fourier coefficients of f_c.

(b) f_c on $2N = 128$.

(c) Fourier reconstruction.

(d) Fourier reconstruction Err. $l^2 = 7.6$

(e) TV reconstruction.

(f) TV reconstruction Err. $l^2 = 6.7$

(g) SPA m=2 reconstruction.

(h) SPA m=2 reconstruction Err. $l^2 = 6.8$

$$f_c(x,y) = \begin{cases} \cos(3\pi\sqrt{x^2+y^2}/2) & \text{if } \sqrt{x^2+y^2} \le \frac{1}{2} \\ \cos(\pi\sqrt{x^2+y^2}/2) & \text{if } \sqrt{x^2+y^2} > \frac{1}{2} \\ \sin(\pi\sqrt{x^2+y^2}/2) & \text{if } 0 < x, y < \frac{3}{4} \end{cases}$$

(i) SPA m=3 reconstruction.

(j) SPA m=3 reconstruction Err. $l^2 = 6.9$

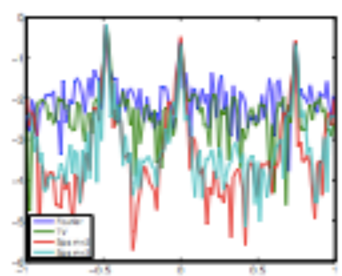

(k) Cross-Section Err. $x = \frac{1}{12}$

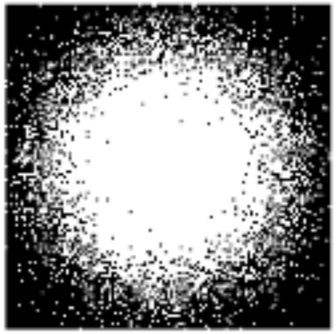

(a) Sampling of 50% of the Fourier coefficients of f_c.

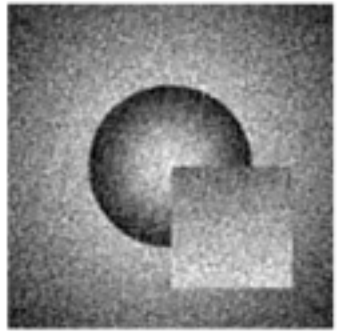

(b) Fourier reconstruction.

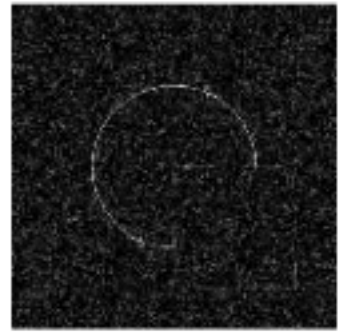

(c) Fourier reconstruction Err. $l^2 = 22.1$

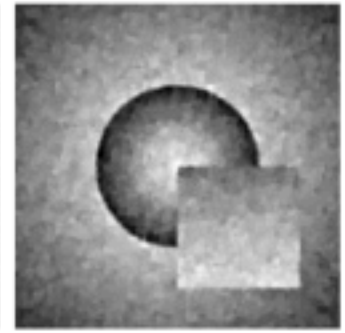

(d) TV reconstruction.

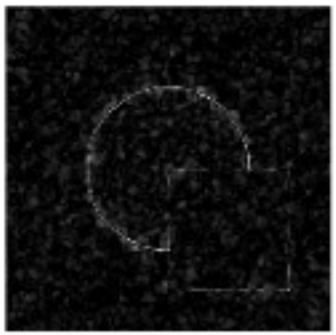

(e) TV reconstruction Err. $l^2 = 14.4$

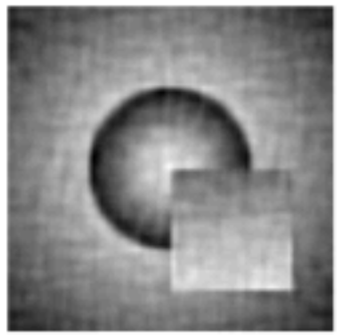

(f) SPA m=2 reconstruction.

(g) SPA m=2 reconstruction Err. $l^2 = 13.0$

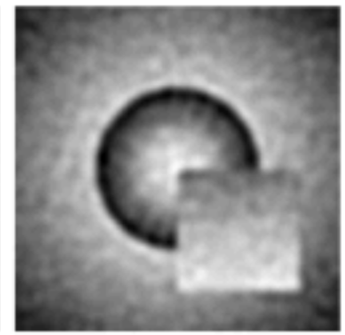

(h) SPA m=3 reconstruction.

(i) SPA m=3 reconstruction Err. $l^2 = 12.8$

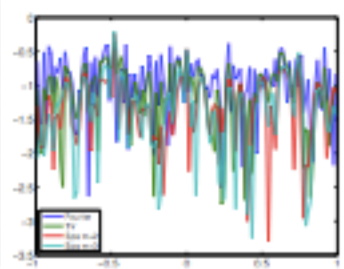

(j) Cross-Section Err. $x = \frac{1}{12}$

High Order Reconstruction for Neutron Tomography

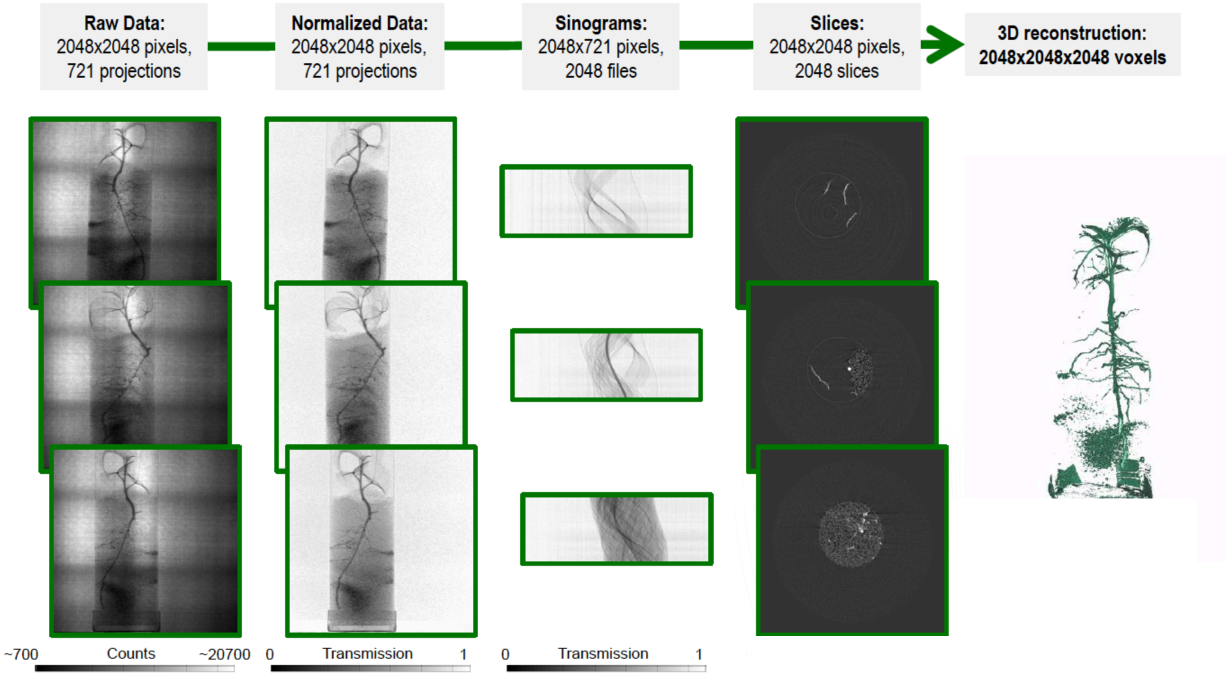

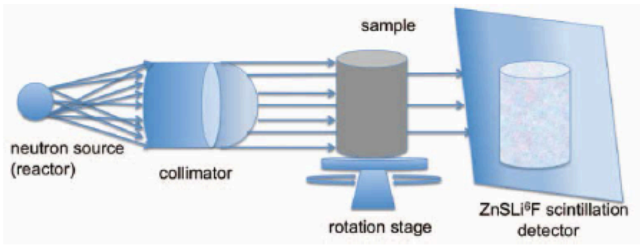

$$\mathcal{M} = \int F(u)\delta\Omega$$

u

Tomography

High Order Reconstruction for Neutron Tomography

$$\mathcal{M} = \int F(u)\delta\Omega$$

$$\min_{\mathbf{u}\in\mathbf{R}^n}\{\|\Phi(\mathbf{u}) - \mathcal{M}_n\|_{\ell^1} + H(\mathbf{u})\}$$

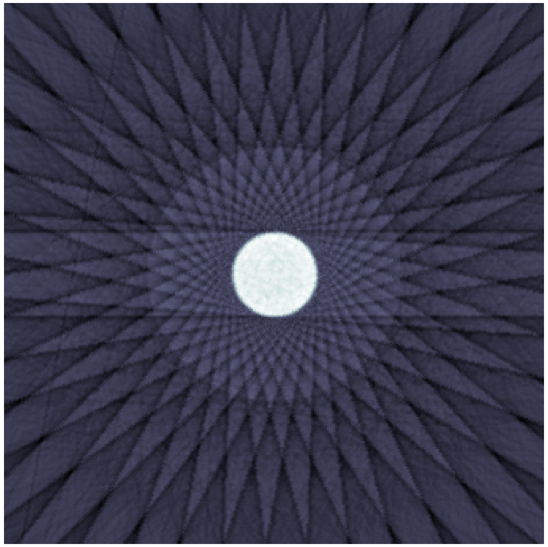

u

- Image is of Aluminum-Steel Phantom taken at HFIR - CG1
- Standard filtered back projection methods in tomographic reconstruction yields artifacts
- Computationally Expensive to reconstruct
- Full 3D dataset is: 2048 ✕ 2048 ✕ 360 ~30GB

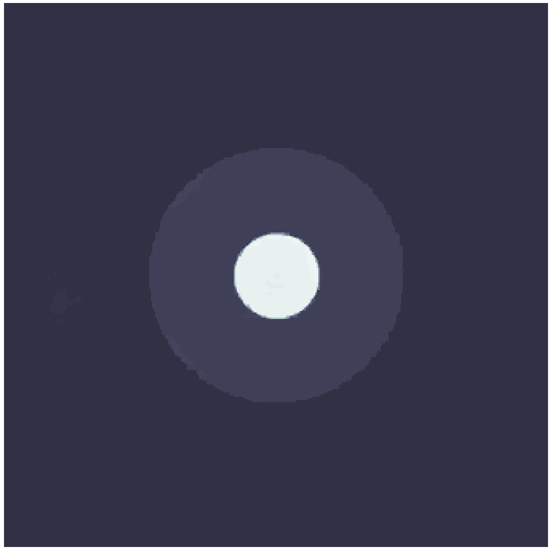

u

High Order Reconstruction for Neutron Tomography

$$\mathcal{M} = \int F(u)\delta\Omega$$

$$\min_{\mathbf{u}\in\mathbf{R}^n} \{\|\Phi(\mathbf{u}) - \mathcal{M}_n\|_{\ell^1} + H(\mathbf{u})\}$$

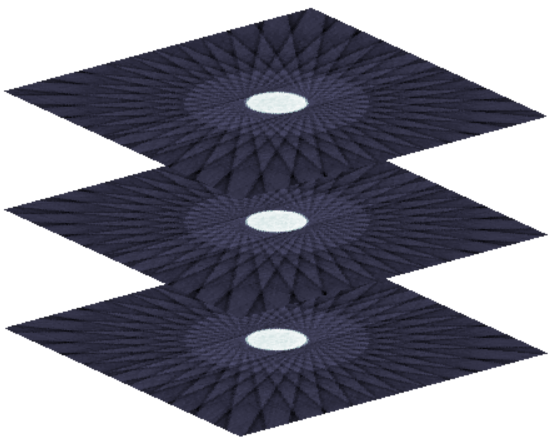

u

- Image is of Aluminum-Steel Phantom taken at HFIR - CG1
- Standard filtered back projection methods in tomographic reconstructi yields artifacts
- Computationally Expensi to reconstruct
- Full 3D dataset is: 2048 ✕ 2048 ✕ 360 ~30G

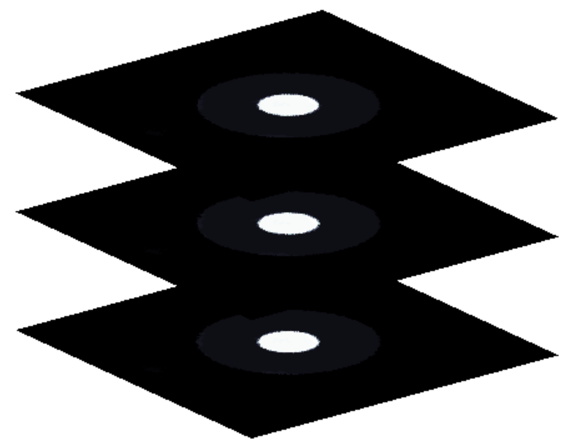

u

High Order Reconstruction for Neutron Tomography

$$\mathcal{M} = \int F(u)\delta\Omega$$

$$\min_{\mathbf{u}\in\mathbf{R}^n}\{\|\Phi(\mathbf{u}) - \mathcal{M}_n\|_{\ell^1} + H(\mathbf{u})\}$$

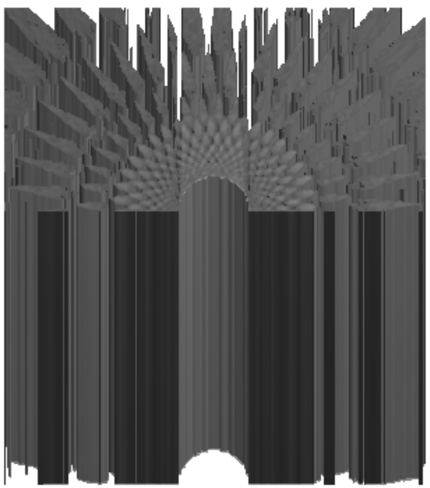

u

- Image is of Aluminum-Steel Phantom taken at HFIR - CG1
- Standard filtered back projection methods in tomographic reconstruction yields artifacts
- Computationally Expensive to reconstruct
- Full 3D dataset is:

2048 ✕ 2048 ✕ 360 ~30GB

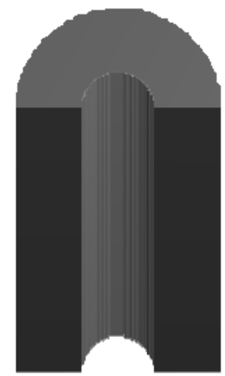

u

Discussion for Long Program

Thank You.